in the presence of IL-2 as a readout. We assume that such a weak self-reactivity of the cells has hampered identifying this potentially important iNKT cell subset in prior studies.

Although we added rIL-2 and IL-15 exogenously to stimulate iNKT cells, these are the cytokines commonly produced in the inflammatory milieu. This allows us to speculate that the IL-5-producing iNKT cells might have a chance to encounter $CD1d^+$ APCs in the presence of either of the cytokines, thereby playing an important role in the local control of inflammation. Interestingly, IL-15 blockade has recently been shown to prevent the induction of allergic airway inflammation (37), implicating indirect evidence for the presence of IL-15 in the site of airway inflammation. Although this study has not identified iNKT cells as a target of IL-15, the critical role of iNKT cells shown in other rodent studies (14, 15) and human asthma (38) supports the idea that local IL-15 may stimulate iNKT cells to produce IL-5 and IL-13, which then leads to augmentation of allergic inflammation involving activation of eosinophils (39, 40). Another point of interest is that the role of IL-2 has been indicated in Th2 polarization processes involving iNKT cells. Although this is most elegantly shown in the case of eradication of certain parasites (41, 42), it is possible that iNKT cells are the target of IL-2 for inducing Th2 polarization. It is also likely that iNKT cells in the inflammatory lesions of MS may produce IL-5 or IL-13 after being triggered by IL-2 or IL-15 in the inflammatory lesions. The IL-5 produced by iNKT cells may directly promote Th2 cell differentiation, thereby deviating Th1/Th2 balance toward Th2. Alternatively, Th2 polarization could be mediated by other cytokines that were triggered by IL-5 in an autocrine or paracrine fashion. In fact, we showed that IL-4 was induced by the IL-5-producing iNKT cells in the presence of IL-5 (Fig. 1*D*) and overproduction of IL-4 from $CD4^+$ iNKT cells could be demonstrated in the remission state of MS (33).

Recent reports have shown that striking Th1 responses against exogenous pathogens could be triggered by iNKT cells after recognizing an endogenous ligand in the presence of IL-12 (26, 31). Given its remarkable homology to the IL-5 response triggered by IL-2 reported here in this article, we speculate that stimulation with an endogenous ligand and locally produced cytokines is a fundamental mechanism that would lead iNKT cells to provoke a decisive response for dealing with infection, allergy, and autoimmunity. In infection models, iNKT cell recognition of iGb3 has been identified as an important trigger for inducing Th1 response by iNKT cells (31). However, iNKT cells may recognize different endogenous Ags (43) and therefore the microenvironment of different tissues or types of inflammation (e.g., Th1 vs Th2) encountered may be instrumental in determining the phenotype of iNKT cytokine production. In this regard, endogenous ligand(s) involved in IL-5 production by IL-2 is an area to be further investigated in the future.

It is important to realize that as much as 8 of the 26 $CD4^+$ iNKT clones (Table I) have demonstrated a bias for IL-5 production following IL-2 stimulation. We speculate that this could arise from the heterogeneity of β-chain CDR3 sequence, although this point is another area that needs to be formally verified. Supportive of this speculation is the recent study showing that individual TCR β-chain may contribute to the variation of Ag recognition among iNKT cells (36). Another possibility is that these IL-5-producing iNKT cells may comprise a distinct lineage with the unique machinery to overproduce IL-5. It may also be due to differences in the frequency of IL-5-biased iNKT cells among each individual. This idea is supported by the observation that IL-5-biased clones tended to be generated from the same individuals (Table I). Furthermore, our preliminary data has demonstrated that IL-2-dependent production from iNKT cells might be subject to mouse strain differences: namely, the production of IL-5 from iNKT cells found in BALB/c could not be demonstrated in C57BL/6 mice (data not shown). This discrepancy between Th1 (C57BL/6) and Th2 (BALB/c) polarized mice may give us an important clue to further analyze this issue.

In summary, the present study has identified presence of human $CD4^+$ iNKT cells that produce IL-5 and IL-13 in response to suboptimal TCR stimulation together with IL-2 or IL-15. Previous studies using αGC or anti-CD3 Ab for stimulation of iNKT cells was unsuccessful in revealing the identity and the unique property of these iNKT cells, reflecting the nonphysiological nature of the methods used for stimulating iNKT cells. Analysis of our data and studies from other groups suggest that this iNKT cell population produce IL-5 and IL-13 in vivo by recognizing an endogenous ligand. In the pathogenesis of allergy, autoimmune diseases or parasite infection, $CD4^+$ iNKT may play a key role in deviating immune responses toward Th2 and thus provide a suitable target for immune intervention. Our results also imply that cytokines could play a major role in instructing the iNKT cell populations to respond differentially in vivo, whether it is beneficial or hazardous. Taking all these into consideration, we propose that sensing the presence of cytokines is probably one of the most fundamental abilities for the iNKT cells that are to be given only a weak TCR signal in vivo.

Acknowledgments

We thank Dr. J. Ludovic Croxford for helpful comments, Yuki Kikai for cell sorting, and Hiromi Yamaguchi for cell culture.

Disclosures

The authors have no financial conflict of interest.

References

1. Bendelac, A., M. Bonneville, and J. F. Kearney. 2001. Autoreactivity by design: innate B and T lymphocytes. *Nat. Rev. Immunol.* 1: 177–186.
2. Taniguchi, M., M. Harada, S. Kojo, T. Nakayama, and H. Wakao. 2003. The regulatory role of Vα14 NKT cells in innate and acquired immune response. *Annu. Rev. Immunol.* 21: 483–513.
3. Wilson, B. S., and T. L. Delovitch. 2003. Janus-like role of regulatory iNKT cells in autoimmune disease and tumour immunity. *Nat. Rev. Immunol.* 3: 211–222.
4. Kronenberg, M. 2005. Toward an understanding of NKT cell biology: progress and paradoxes. *Annu. Rev. Immunol.* 23: 877–900.
5. Kawano, T., J. Cui, Y. Koezuka, Y. Toura, Y. Kaneko, K. Motoki, H. Ueno, R. Nakagawa, H. Sato, E. Kondo, et al. 1997. CD1d-restricted and TCR-mediated activation of Vα14 NKT cells by glycosylceramides. *Science* 278: 1626–1629.
6. Godfrey, D. I., H. R. MacDonald, M. Kronenberg, M. J. Smyth, and L. van Kaer. 2004. NKT cells: what's in a name? *Nat. Rev. Immunol.* 4: 231–237.
7. Duarte, N., M. Stenstrom, S. Campino, M. L. Bergman, M. Lundholm, D. Holmberg, and S. L. Cardell. 2004. Prevention of diabetes in nonobese diabetic mice mediated by CD1d-restricted nonclassical NKT cells. *J. Immunol.* 173: 3112–3118.
8. Terabe, M., J. Swann, E. Ambrosino, P. Sinha, S. Takaku, Y. Hayakawa, D. I. Godfrey, S. Ostrand-Rosenberg, M. J. Smyth, and J. A. Berzofsky. 2005. A nonclassical non-Vα14-Jα18 CD1d-restricted (type II) NKT cell is sufficient for down-regulation of tumor immunosurveillance. *J. Exp. Med.* 202: 1627–1633.
9. Gumperz, J. E., S. Miyake, T. Yamamura, and M. B. Brenner. 2002. Functionally distinct subsets of CD1d-restricted natural killer T cells revealed by CD1d tetramer staining. *J. Exp. Med.* 195: 625–636.
10. Lee, P. T., K. Benlagha, L. Teyton, and A. Bendelac. 2002. Distinct functional lineages of human Vα24 natural killer T cells. *J. Exp. Med.* 195: 637–641.
11. Kim, H. Y., H. J. Kim, H. S. Min, S. Kim, W. S. Park, S. H. Park, and D. H. Chung. 2005. NKT cells promote antibody-induced joint inflammation by suppressing transforming growth factor β1 production. *J. Exp. Med.* 201: 41–47.
12. Chiba, A., S. Kaieda, S. Oki, T. Yamamura, S. Miyake, and 2005. The involvement of Vα14 NKT cells in the pathogenesis of arthritis in murine models. *Arthritis Rheum.* 52: 1941–1948.
13. Ohnishi, Y., A. Tsutsumi, D. Goto, S. Itoh, I. Matsumoto, M. Taniguchi, and T. Sumida. 2005. TCR Vα14 natural killer T cells function as effector T cells in mice with collagen-induced arthritis. *Clin. Exp. Immunol.* 141: 47–53.
14. Akbari, O., P. Stock, E. Meyer, M. Kronenberg, S. Sidobre, T. Nakayama, M. Taniguchi, M. J. Grusby, R. H. DeKruyff, and D. T. Umetsu. 2003. Essential role of NKT cells producing IL-4 and IL-13 in the development of allergen-induced airway hyperreactivity. *Nat. Med.* 9: 582–588.
15. Lisbonne, M., S. Diem, A. de Castro Keller, J. Lefort, L. M. Araujo, P. Hachem, J.-M. Fourneau, S. Sidobre, M. Kronenberg, M. Taniguchi, et al. 2003. Cutting

edge: invariant Vα14 NKT cells are required for allergen-induced airway inflammation and hyperreactivity in an experimental asthma model. *J. Immunol.* 171: 1637–1641.
16. Godfrey, D. I., and M. Kronenberg. 2004. Going both ways: immune regulation via CD1d-dependent NKT cells. *J. Clin. Invest.* 114: 1379–1388.
17. Chen, H., and W. E. Paul. 1997. Cultured NK1.1$^+$CD4$^+$ T cells produce large amounts of IL-4 and IFN-γ upon activation by anti-CD3 or CD1. *J. Immunol.* 159: 2240–2249.
18. Schmieg, J., G. Yang, R. W. Franck, and M. Tsuji. 2003. Superior protection against malaria and melanoma metastases by a c-glycoside analogue of the natural killer T cell ligand α-galactosylceramide. *J. Exp. Med.* 198: 1631–1641.
19. Miyamoto, K., S. Miyake, and T. Yamamura. 2001. A synthetic glycolipid prevents autoimmune encephalomyelitis by inducing Th2 bias of natural killer T cells. *Nature* 413: 531–534.
20. Miyake, S., and T. Yamamura. 2005. Therapeutic potential of glycolipid ligands for natural killer (NK) T cells in the suppression of autoimmune disease. *Curr. Drug Targets Immune Endocr. Metabol. Disord.* 5: 315–322.
21. Heller, F., I. J. Fuss, E. E. Nieuenhuis, R. S. Blumberg, and W. Strober. 2002. Oxazolone colitis, a Th2 colitis model resembling ulcerative colitis, is mediated by IL-13-producing NK-T cells. *Immunity* 17: 629–638.
22. D'Andrea, A., D. Goux, C. De Lalla, Y. Koezuka, D. Montagna, A. Moretta, P. Dellabona, G. Casorati, and S. Abrignani. 2000. Neonatal invariant Vα24$^+$ NKT lymphocytes are activated memory cells. *Eur. J. Immunol.* 30: 1544–1550.
23. Park, S. H., K. Benlagha, D. Lee, E. Balish, and A. Bendelac. 2000. Unaltered phenotype of, tissue distribution and function of Vα14$^+$ NKT cells in germ-free mice. *Eur. J. Immunol.* 30: 620–625.
24. Matsuda, J. L., L. Gapin, J. L. Baron, S. Sidobre, D. B. Stetson, M. Mohrs, R. M. Locksley, and M. Kronenberg. 2003. Mouse Vα14i natural killer T cells are resistant to cytokine polarization in vivo. *Proc. Natl. Acad. Sci. USA* 100: 8395–8400.
25. Oki, S., A. Chiba, T. Yamamura, and S. Miyake. 2004. The clinical implication and molecular mechanism of preferential IL-4 production by modified glycolipid-stimulated NKT cells. *J. Clin. Invest.* 113: 1631–1640.
26. Brigl, M., L. Bry, S. C. Kent, J. E. Gumperz, and M. B. Brenner. 2003. Mechanism of CD1d-restricted natural killer T cell activation during microbial infection. *Nat. Immunol.* 4: 1230–1236.
27. Joyce, S., A. S. Woods, J. W. Yewdell, J. R. Bennink, D. De Silva, A. Boesteanu, S. P. Balk, R. J. Cotter, and R. R. Brutkiewicz. 1998. Natural ligand of mouse CD1d1: cellular glycosylphosphatidylinositol. *Science* 279: 1541–1544.
28. Gumperz, J. E., C. Roy, A. Makowska, D. Lum, M. Sugita, T. Podrebarac, Y. Koezuka, S. Porcelli, S. Cardell, M. B. Brenner, and S. M. Behar. 2000. Murine CD1d-restricted T cell recognition of cellular lipids. *Immunity* 12: 211–221.
29. Rauch, J., J. E. Gumperz, C. Robinson, M. Skold, C. Roy, D. C. Young, M. Lafler, B. D. Moody, M. B. Brenner, and C. E. Costello. 2003. Structural features of the acyl chain determine self-phospholipid antigen recognition by a CD1d-restricted invariant NKT (iNKT) cell. *J. Biol. Chem.* 278: 47508–47515.
30. Zhou, D., J. Mattner, C. Cantu, 3rd, N. Schrantz, N. Yin, Y. Gao, Y. Sagiv, K. Hudspeth, Y. Wu, T. Yamashita, et al. 2004. Lysosomal glycosphingolipid recognition by NKT cells. *Science* 306: 1786–1789.
31. Mattner, J., K. L. Debord, N. Ismail, R. D. Goff, C. Cantu, 3rd, D. Zhou, P. Saint-Mezard, V. Wang, Y. Gao, N. Yin, et al. 2005. Exogenous and endogenous glycolipid antigens activate NKT cells during microbial infections. *Nature* 434: 525–529.
32. Thomas, S. Y., R. Hou, J. E. Boyson, T. K. Means, C. Hess, D. P. Olson, J. L. Strominger, M. B. Brenner, J. E. Gumperz, S. B. Wilson, and A. D. Luster. 2003. CD1d-restricted NKT cells express a chemokine receptor profile indicative of Th1-type inflammatory homing cells. *J. Immunol.* 171: 2571–2580.
33. Araki, M., T. Kondo, J. E. Gumperz, M. B. Brenner, S. Miyake, and T. Yamamura. 2003. Th2 bias of CD4$^+$ NKT cells derived from multiple sclerosis in remission. *Int. Immunol.* 15: 279–288.
34. Takahashi, K., T. Aranami, M. Endoh, S. Miyake, and T. Yamamura. 2004. The regulatory role of natural killer cells in multiple sclerosis. *Brain* 127: 1917–1927.
35. van Der Vliet, H. J., N. Nishi, T. D. de Gruijl, B. M. van Blomberg, A. J. van den Eertwegh, H. M. Pinedo, G. Giaccone, and R. J. Scheper. 2000. Human natural killer T cells acquire a memory-active phenotype before birth. *Blood* 95: 2440–2442.
36. Brigl, M., P. van den Elzen, X. Chen, J. H. Meyers, D. Wu, C.-H. Wong, F. Reddington, P. A. Illarianov, G. S. Besra, M. B. Brenner, and J. E. Gumperz. 2006. Conserved and heterogeneous lipid antigen specificities of CD1d-restricted NKT cell receptors. *J. Immunol.* 176: 3625–3634.
37. Ruckert, R., K. Brandt, A. Braun, H.-G. Hoymann, U. Herz, V. Budagian, H. Durkop, H. Renz, and S. Bulfone-Paus. 2005. Blocking IL-15 prevents the induction of allergen-specific T cells and allergic inflammation in vivo. *J. Immunol.* 174: 5507–5515.
38. Akbari, O., J. L. Faul, J. L. Hoyte, G. J. Berry, J. Wahlstrom, M. Kronenberg, R. H. DeKruyff, and D. T. Umetsu. 2006. CD4$^+$ invariant T-cell-receptor$^+$ natural killer T cells in bronchial asthma. *N. Engl. J. Med.* 354: 1117–1129.
39. Yamaguchi, Y., T. Suda, J. Suda, M. Eguchi, Y. Miura, N. Harada, A. Tominaga, and K. Takatsu. 1988. Purified interleukin 5 supports the terminal differentiation and proliferation of murine eosinophilic precursors. *J. Exp. Med.* 167: 43–56.
40. Yamaguchi, Y., Y. Hayashi, Y. Sugama, Y. Miura, T. Kasahara, S. Kitamura, M. Torisu, S. Mita, A. Tominaga, and K. Takatsu. 1988. Highly purified murine interleukin (IL-5) stimulates eosinophil function and prolongs in vitro survival: IL-5 as eosinophil chemotactic factor. *J. Exp. Med.* 167: 1737–1742.
41. Cui, J., N. Watanabe, T. Kawano, M. Yamashita, T. Kamata, C. Shimizu, M. Kimura, E. Shimizu, J. Koike, H. Koseki, et al. 1999. Inhibition of T helper cell type 2 cell differentiation and immunoglobulin E response by ligand-activated Vα14 natural killer T cells. *J. Exp. Med.* 190: 783–792.
42. Mallevaey, T., J. P. Zanetta, C. Faveeuw, J. Fontain, E. Maes, F. Platt, M. Capron, M. L. de-Moraes, and F. Trottein. 2006. Activation of invariant NKT cells by the helminth parasite *Schistosoma mansoni*. *J. Immunol.* 176: 2476–2485.
43. Porubsky, S., A. O. Speak, B. Luckow, V. Cerundolo, F. M. Platt, and H.-J. Grone. 2007. Normal development and function of invariant natural killer T cells in mice with isoglobosylceramide (iGb3) deficiency. *Proc. Natl. Acad. Sci. USA* 104: 5977–5982.

nature medicine

Direct suppression of CNS autoimmune inflammation via the cannabinoid receptor CB_1 on neurons and CB_2 on autoreactive T cells

Katarzyna Maresz[1,11], Gareth Pryce[2,10,11], Eugene D Ponomarev[1], Giovanni Marsicano[3], J Ludovic Croxford[2,4], Leah P Shriver[1,5], Catherine Ledent[6], Xiaodong Cheng[1], Erica J Carrier[7], Monica K Mann[1,5], Gavin Giovannoni[2,10], Roger G Pertwee[8], Takashi Yamamura[4], Nancy E Buckley[9], Cecilia J Hillard[7], Beat Lutz[3], David Baker[2,10,11] & Bonnie N Dittel[1,5,11]

The cannabinoid system is immunomodulatory and has been targeted as a treatment for the central nervous system (CNS) autoimmune disease multiple sclerosis. Using an animal model of multiple sclerosis, experimental autoimmune encephalomyelitis (EAE), we investigated the role of the CB_1 and CB_2 cannabinoid receptors in regulating CNS autoimmunity. We found that CB_1 receptor expression by neurons, but not T cells, was required for cannabinoid-mediated EAE suppression. In contrast, CB_2 receptor expression by encephalitogenic T cells was critical for controlling inflammation associated with EAE. CB_2-deficient T cells in the CNS during EAE exhibited reduced levels of apoptosis, a higher rate of proliferation and increased production of inflammatory cytokines, resulting in severe clinical disease. Together, our results demonstrate that the cannabinoid system within the CNS plays a critical role in regulating autoimmune inflammation, with the CNS directly suppressing T-cell effector function via the CB_2 receptor.

Although the central nervous system (CNS) has been considered an immune-privileged site, it is now appreciated that activated T lymphocytes can enter the CNS without causing damage[1]. It is not known how these pro-inflammatory T cells are controlled within the CNS. In the human autoimmune disease multiple sclerosis, myelin-specific T cells can overcome the CNS protective microenvironment and cause inflammation, resulting in demyelinated plaques and neurological symptoms[2]. Most multiple sclerosis patients exhibit a relapsing and remitting course of the disease; however, the mechanisms involved in resolving inflammation during remission, including the elimination of autoreactive T cells, is not well understood[2]. Treatments for multiple sclerosis have included cannabinoid agonists, such as delta(9)-tetrahydrocannabinol (THC), which function by signaling through the cannabinoid receptors CB_1 and CB_2 (refs. 3,4). The CB_1 receptor is expressed at a high level by most neurons and at a lower level by immune cells[3,5]. In contrast, the CB_2 receptor is highly expressed by immune cells[6] and by some neurons in the brain stem[7]. Both receptors bind the endocannabinoid lipid mediators anandamide (AEA) and 2-archidonoylglycerol (2-AG)[8]. The cannabinoid system has been shown to be immune regulatory, altering cell proliferation, suppressing immune cell activation and cytokine production, and enhancing apoptosis[6]. Cannabinoids improve clinical disease not only in humans with multiple sclerosis[9], but also in rodent models of EAE (refs. 10–12). In the current study, we separate the roles of the CB_1 and CB_2 receptors on T cells and neurons.

We previously reported a role for the CB_1 receptor in neuroprotection during EAE; however, that study did not examine the influence cannabinoids have on immune aspects of disease[13]. To examine this question, we first determined that ABH mice were susceptible to suppression of EAE via cannabinoid receptor signaling, by administering THC, a CB_1 and CB_2 receptor agonist, from days 10 to 22 after EAE induction (**Fig. 1a** and **Table 1**). We found that a THC dose of 10 mg per kg (body weight) was sufficient to significantly inhibit the severity of clinical disease ($P < 0.05$), as indicated by a reduced maximal clinical score and a delay in EAE onset (**Fig. 1a** and **Table 1**). Cannabidiol (CBD), a cannabinoid with no CB_1 or CB_2 receptor agonist activity, did not alter EAE clinical disease (**Table 1**), and mice lacking the CB_1 receptor (ABH·$CB_1^{-/-}$) were not susceptible to THC-mediated inhibition of EAE (**Table 1**).

[1]BloodCenter of Wisconsin, Blood Research Institute, Milwaukee, Wisconsin 53226, USA. [2]Department of Neuroinflammation, Institute of Neurology, University College London, London WC1N 1PJ, UK. [3]Department of Physiological Chemistry, Johannes Gutenberg-University Mainz, 55099 Mainz, Germany. [4]Department of Immunology, National Institute of Neuroscience, Tokyo 187-8502, Japan. [5]Department of Microbiology and Molecular Genetics, Medical College of Wisconsin, Milwaukee, Wisconsin 53226, USA. [6]Institut de Recherche Interdisciplinaire en Biologie Humaine et Moleculaire, Université libre de Bruxelles, B-1070 Brussels, Belgium. [7]Department of Pharmacology and Toxicology, Medical College of Wisconsin, Milwaukee, Wisconsin 53226, USA. [8]Department of Biomedical Sciences, Institute of Medical Sciences, University of Aberdeen, Aberdeen AB25 2ZD, UK. [9]Biological Sciences Department, California State Polytechnic University, Pomona, California 91768, USA. [10]Present address: Neuroimmunology Unit, Neuroscience Centre, Institute of Cell and Molecular Science, Barts and the London School of Medicine and Dentistry, Queen Mary University of London, London E1 2AT, UK. [11]These authors contributed equally to this work. Correspondence should be addressed to B.N.D. (bonnie.dittel@bcw.edu).

Received 23 June 2006; accepted 23 February 2007; published online 1 April 2007; doi:10.1038/nm1561

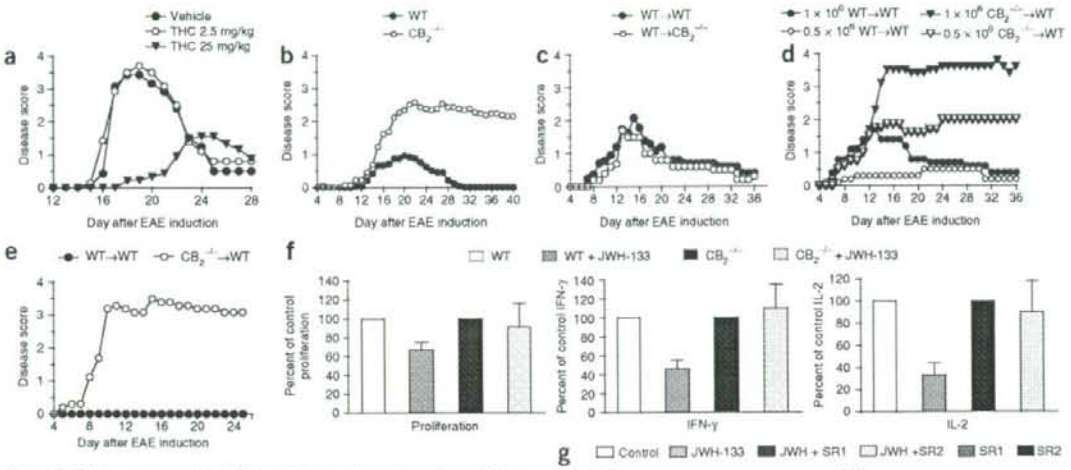

Figure 1 EAE is suppressed by THC in wild-type mice and is enhanced when induced with $CB_2^{-/-}$ T cells, which, unlike $CB_1^{-/-}$ T cells, are not responsive to the CB_2 receptor agonist JWH-133. (**a**) EAE was induced in ABH mice by active immunization. Typically, on days 10–22 the mice were treated with injections of vehicle, 2.5 mg/kg THC or 25 mg/kg THC. (**b**) EAE was induced by immunization with Ac1-11 peptide of 12 wild-type and 13 $CB_2^{-/-}$ mice in three groups. (**c–e**) EAE was induced in either B10.PL or $CB_2^{-/-}$ mice by the adoptive transfer of either 0.5 or 1×10^6 wild-type or $CB_2^{-/-}$ encephalitogenic T cells. Each experiment was performed three times with 3–5 mice per group. (**e**) EAE was induced as in **d** without irradiation. In **a–e**, data shown is the average daily disease scores from all the mice. (**f**) Wild-type and $CB_2^{-/-}$ myelin basic protein (MBP)-specific encephalitogenic T cells were activated *in vitro* with Ac1-11 peptide. (**g**) Hen egg lysozyme (HEL)-specific wild-type and $CB_1^{-/-}$ T cells were harvested from draining lymph nodes 10 d after immunization and activated with HEL. (**f,g**) Seven days following activation, the T cells were reactivated with Ac1-11 or HEL in the presence of vehicle alone, 200 nM JWH-133, JWH-133 and 500 nM SR1 or SR2, SR1 alone or SR2 alone. Proliferation was measured by BrdU incorporation, and real-time PCR was used to detect IFN-γ and IL-2. Vehicle control levels of proliferation and cytokine production in both wild-type and $CB_2^{-/-}$ T cells were not substantially different, so they were set at 100%, and the treated groups are shown as the percent response of the appropriate control ± s.d. of three replicates.

To differentiate between CB_1 expression in the nervous and immune systems, we generated conditional knockout mice with a CB_1 receptor deficiency in either T cells (ABH·$CB_1^{-/f}$·Tg(*Lck-cre*)) or neurons (ABH·$CB_1^{-/f}$·Tg(*Nes-cre*)). Upon treatment with vehicle, mice lacking the CB_1 receptor specifically in T cells or neurons had similar EAE clinical disease as compared to the ABH and ABH·$CB_1^{0/f}$ control mice (**Table 1**). However, upon treatment with THC, a deficiency in neuronal, but not T-cell, CB_1 receptor expression abolished THC-mediated EAE suppression. These data demonstrate that the CB_1 receptor does not play a role in the regulation of CNS autoimmunity in the steady state but that its expression on neurons is important for the efficacy of cannabinoid-based agonist therapies. In addition, these data show that T-cell CB_1 receptor expression is dispensable for regulation of EAE.

To determine whether the CB_2 receptor plays a role in the regulation of CNS autoimmunity, we induced EAE in wild-type and CB_2-deficient ($CB_2^{-/-}$) B10.PL mice by active immunization. As compared to wild-type mice, we found that $CB_2^{-/-}$ mice exhibited a higher incidence of disease, a significantly increased clinical score and a reduced recovery rate ($P < 0.001$) (**Fig. 1b** and **Supplementary Table 1** online). These data demonstrate that unlike the CB_1 receptor, the CB_2 receptor is an important regulator of EAE clinical disease in the steady state. To identify the critical CB_2 receptor–expressing cell(s), we induced EAE with either wild-type or $CB_2^{-/-}$ encephalitogenic T cells by adoptive transfer of 1×10^6 T cells into either wild-type or $CB_2^{-/-}$ mice. EAE induced by wild-type T cells was similar in both wild-type and $CB_2^{-/-}$ mice (**Fig. 1c**). However, when we performed the reciprocal experiment, mice with EAE induced by $CB_2^{-/-}$ T cells exhibited more severe clinical disease that was characterized by a higher mortality rate and the presence of increased numbers of infiltrating mononuclear cells (**Fig. 1d** and **Table 2**). These data show that CB_2 receptor expression by encephalitogenic T cells, and not CNS tissue, is important for the regulation of CNS autoimmunity.

To further demonstrate the enhanced potency of $CB_2^{-/-}$ encephalitogenic T cells in EAE induction, we induced EAE with 0.5×10^6 T cells. This number of wild-type T cells induced either no disease or a very mild disease; however, the same number of $CB_2^{-/-}$ encephalitogenic T cells induced a chronic disease course (**Fig. 1d**). In the adoptive transfer model of EAE induction, irradiation of recipient mice increases the efficiency of EAE induction; however, $CB_2^{-/-}$ T cells were just as effective at inducing EAE without irradiation (**Fig. 1e**).

As EAE induced with $CB_2^{-/-}$ T cells was more severe, this suggested that encephalitogenic CD4 T-cell effector functions are regulated via the CB_2 receptor. To examine this possibility, we reactivated wild-type T cells *in vitro* and measured proliferation and production of the T-helper type 1 (T_H1) cytokines interferon (IFN)-γ and interleukin (IL)-2. The addition of the CB_2 receptor agonist JWH-133 resulted in an ~40% reduction in proliferation of wild-type T cells and an ~60% reduction in production of both cytokines (**Fig. 1f**). In contrast, JWH-133 did not alter proliferation or cytokine production

Table 1 Immunosuppression in EAE in ABH mice by cannabinoids is mediated by CB_1 receptor expressed in the CNS

Strain[a]	CB_1 genotype[b] T cell	CB_1 genotype[b] CNS	Treatment[c]	Dose	No. EAE/total[d]	Group score ± s.e.m.[e]	EAE score ± s.e.m.[f]	Day of onset ± s.d.[g]
WT normal mouse								
ABH WT	+/+	+/+	Untreated		26/26	3.9 ± 0.1	3.9 ± 0.1	17.1 ± 1.6
ABH WT	+/+	+/+	Vehicle		8/8	3.8 ± 0.1	3.8 ± 0.1	16.5 ± 0.9
ABH WT	+/+	+/+	THC	0.25 mg/kg	9/9	3.8 ± 0.1	3.8 ± 0.1	16.2 ± 2.0
ABH WT	+/+	+/+	THC	2.5 mg/kg	10/10	3.8 ± 0.1	3.8 ± 0.1	17.5 ± 1.9
ABH WT	+/+	+/+	THC	25 mg/kg	7/9	1.7 ± 0.4**	2.1 ± 0.3**	20.7 ± 1.8**
ABH WT	+/+	+/+	Vehicle		9/10	3.6 ± 0.4	3.9 ± 0.1	15.2 ± 0.8
ABH WT	+/+	+/+	THC	10 mg/kg	6/7	2.3 ± 0.6*	3.1 ± 0.5**	17.2 ± 1.8**
ABH WT	+/+	+/+	THC	20 mg/kg	2/8	0.8 ± 0.5***	3.0 ± 0.0	16.0 ± 1.8**
ABH WT	+/+	+/+	Untreated		11/12	3.3 ± 0.4	3.6 ± 0.2	16.2 ± 1.3
ABH WT	+/+	+/+	CBD	0.5 mg/kg	10/10	3.7 ± 0.2	3.7 ± 0.2	16.5 ± 1.2
ABH WT	+/+	+/+	CBD	5.0 mg/kg	8/10	3.0 ± 0.5	3.8 ± 0.1	16.9 ± 1.2
ABH WT	+/+	+/+	Untreated	6/11	12/12	3.8 ± 0.4	3.8 ± 0.2	14.9 ± 1.2
ABH WT	+/+	+/+	CBD	10 mg/kg	7/7	4.0 ± 0.0	4.0 ± 0.0	14.8 ± 1.8
ABH WT	+/+	+/+	CBD	25 mg/kg	8/8	4.0 ± 0.0	4.0 ± 0.0	15.1 ± 0.4
Generalized CB_1 knockout								
ABH.$CB_1^{-/-}$	+/+	+/+	Untreated		6/6	4.0 ± 0.0	4.0 ± 0.0	15.9 ± 1.2
ABH.$CB_1^{+/-}$	+/–	+/–	Untreated		7/7	4.0 ± 0.0	4.0 ± 0.0	17.0 ± 0.8
ABH.$CB_1^{-/-}$	–/–	–/–	Untreated		10/10	4.0 ± 0.0	4.0 ± 0.0	18.0 ± 1.8
ABH.$CB_1^{+/-}$	+/–	+/–	Vehicle		9/9	4.2 ± 0.2	4.2 ± 0.2	15.9 ± 1.2
ABH.$CB_1^{+/-}$	+/–	+/–	THC	20 mg/kg	4/8	1.3 ± 0.6**	2.6 ± 0.6**	17.0 ± 0.8
ABH.$CB_1^{-/-}$	–/–	–/–	THC	20 mg/kg	5/6	3.0 ± 0.8	3.6 ± 0.6	18.0 ± 1.8
Conditional CB_1 knockout								
ABH WT	+/+	+/+	Untreated		9/9	3.6 ± 0.1	3.6 ± 0.1	15.4 ± 1.1
ABH.$CB_1^{f/f}$	+/+	+/+	Untreated		6/6	3.3 ± 0.2	3.3 ± 0.2	15.0 ± 0.6
ABH.CB_1^{-f}.Tg(*Lck-cre*)$^{-/+}$	–/–	+/–	Vehicle		6/8	2.9 ± 0.6	3.9 ± 0.1	16.2 ± 1.3
ABH.CB_1^{-f}.Tg(*Lck-cre*)$^{-/-}$	+/–	+/–	Vehicle		7/7	4.0 ± 0.0	4.0 ± 0.0	15.7 ± 1.3
ABH.CB_1^{-f}.Tg(*Nes-cre*)$^{-/-}$	+/–	+/–	Vehicle		19/21	3.5 ± 0.3	3.8 ± 0.2	15.5 ± 1.5
ABH.CB_1^{-f}.Tg(*Nes-cre*)$^{-/+}$	+/–	–/–	Vehicle		24/27	3.5 ± 0.2	3.9 ± 0.1	15.3 ± 1.3
ABH.CB_1^{-f}.Tg(*Lck-cre*)$^{-/+}$	–/–	+/–	THC	20 mg/kg	7/16	0.8 ± 0.3**	1.8 ± 0.4**	16.7 ± 1.4
ABH.CB_1^{-f}.Tg(*Lck-cre*)$^{-/-}$	+/–	+/–	THC	20 mg/kg	6/11	0.8 ± 0.4***	1.5 ± 0.5**	16.5 ± 1.3
ABH.CB_1^{-f}.Tg(*Nes-cre*)$^{-/+}$	+/–	+/–	THC	20 mg/kg	14/20	1.3 ± 0.3***	1.9 ± 0.4***	15.7 ± 0.8
ABH.CB_1^{-f}.Tg(*Nes-cre*)$^{-/+}$	+/–	–/–	THC	20 mg/kg	7/9	2.7 ± 0.5	3.4 ± 0.2	15.0 ± 0.8

[a]Mice that were either homozygous for the null-expressing CB_1 construct ($CB_1^{-/-}$) or littermates from crosses between *Cre* transgene heterozygotes and mice homozygous for the 'floxed' CB_1 construct ($CB_1^{f/f}$) were injected with mouse spinal cord homogenate in Freund's adjuvant on days 0 and 7 to induce EAE. [b]The CB_1 (*Cnr1*) genotype in T cells or the CNS is indicated for each strain. [c]Mice were injected intraperitoneally daily from day 10 to day 22 with compounds dissolved in ethanol:cremaphor:PBS or DMSO:PBS. [d]Data shown is the number of mice that developed EAE of the total number of immunized mice. [e]The results indicate the mean maximal clinical score of all the mice in the group. [f]The results indicate the mean maximal clinical score of the animals that developed EAE. [g]The results indicate the mean day on which mice exhibited clinical signs of EAE.*$P < 0.05$, **$P < 0.01$, ***$P < 0.001$ compared to relevant vehicle-treated controls.

by $CB_2^{-/-}$ T cells (**Fig. 1f**). These data indicate that wild-type T-cell effector functions are inhibited via the CB_2 receptor.

We also confirmed that a deficiency in the CB_1 receptor did not alter responsiveness through the CB_2 receptor. Using antigen-specific T-cell lines generated from $CB_1^{-/-}$ mice, we found that proliferation of both wild-type and knockout T cells was inhibited by JWH-133 (**Fig. 1g**). This activity was mediated through the CB_2 receptor, as the CB_2 receptor–selective antagonist SR144528 (SR2)[14], but not the CB_1 receptor antagonist SR141716 (SR1)[15], blocked JWH-133–mediated inhibition of proliferation in both wild-type and $CB_1^{-/-}$ mice (**Fig. 1g**). Neither SR1 nor SR2 produced an effect when added alone to the cells (**Fig. 1g**). These data indicate that the CB_1 receptor does not modulate T-cell effector function via cross-talk with the CB_2 receptor.

To determine whether differences in inflammatory lesions could explain the more severe disease, we performed histology, and found no

Table 2 Summary of the disease course and cell parameters on day 13 after EAE induction using wild-type or $CB_2^{-/-}$ encephalitogenic T cells

	WT → WT	$CB_2^{-/-}$ → WT	*P*-value[e]
Number of animals	25	25	
Mortality[a]	0%	16%	
Average clinical score[b]	1.26 ± 0.05	1.7 ± 0.2	0.02
Mononuclear cells (× 10^3)[c]	293 ± 41	486 ± 17	0.13
Encephalitogenic T cells (× 10^3)[d]	36 ± 5	58 ± 11	0.03
Myeloid cells (× 10^3)[d]	206 ± 48	335 ± 15	0.24

[a]The percentage of deceased mice on day 13 after EAE induction. [b]Graded disease score as described in Materials and Methods. [c]The absolute number was determined by dividing the total cell count (obtained by counting on a hemocytometer) by the number of mice in each group. [d]The absolute number of infiltrating encephalitogenic T cells and myeloid cells was determined by multiplying the total cell count (obtained by counting on a hemocytometer) by the percentage of cells determined as $CD4^+$ and $V\beta8.2^+$ or $CD11b^+$ (by flow cytometry), and then dividing by the number of mice in each group. The data shown are the average ± s.d. of three experiments with at least seven mice per group. [e]The *P*-value was calculated between the WT → WT and $CB_2^{-/-}$ → WT groups.

difference in the number or size of lesions between the two groups of mice. However, we did observe an increase in T cells in and around the lesions when EAE was induced with $CB_2^{-/-}$ T cells (**Fig. 2a**), which was confirmed by measuring the absolute number of encephalitogenic T cells in the CNS (significantly increased: $P = 0.03$) (**Fig. 2b** and **Table 2**). However, neither the absolute number of total CNS mononuclear cells nor the number of myeloid cells was increased (**Table 2**). Contrary to the increase in encephalitogenic T cells in the CNS (**Fig. 2b**), the number of T cells in the spleen was not affected (**Fig. 2b**), indicating a CNS-specific role for the CB_2 receptor on T cells during EAE.

Because both natural and synthetic cannabinoids are known to have immunosuppressive properties associated with induction of apoptosis and inhibition or suppression of lymphocyte proliferation[16,17], we investigated whether either of these was disrupted in $CB_2^{-/-}$ T cells. We found a 50% increase in the number of proliferating $CB_2^{-/-}$ T cells in the CNS compared to wild-type T cells (**Fig. 2c**), whereas 50% fewer $CB_2^{-/-}$ T cells were apoptotic (**Fig. 2d**). In the spleen, no differences in proliferation (**Fig. 2c**) or apoptosis (**Fig. 2d**) were observed, providing further evidence that the CNS actively suppresses T-cell function through the CB_2 receptor.

Cannabinoids have been shown to modulate cytokine production in immune cells in a concentration-dependent manner. Autoreactive T cells in both EAE and multiple sclerosis express pro-inflammatory cytokines, including IL-2, IFN-γ and granulocyte macrophage–colony stimulating factor (GM-CSF). Whereas these cytokines are barely detectable in the normal CNS, they are rapidly upregulated during EAE (refs. 18,19). Using real-time RT-PCR, we found that when EAE was induced by CB_2-deficient T cells, the level of both *Il2* and *Ifng* in the spinal cord was increased tenfold compared with EAE induction by wild-type T cells (**Fig. 2e**), a difference not seen in the spleen (**Fig. 2f**). We observed a similar trend for *Csf2* gene expression in the spinal cord (**Fig. 2e**) and saw little difference in the spleen (**Fig. 2f**). We next asked whether the increase in T_H1 cytokines was due to increased numbers of cytokine-producing $CB_2^{-/-}$ T cells in the CNS or whether individual T cells were producing more cytokines. Thus, we sorted both wild-type and $CB_2^{-/-}$ encephalitogenic T cells from the CNS of mice with EAE, and measured IL-2 and GM-CSF production. We found that the production of both *Il2* and *Csf2* mRNA was significantly increased in the $CB_2^{-/-}$ encephalitogenic T cells as compared to wild-type T cells ($P < 0.05$) (**Fig. 2g**). *Ifng*

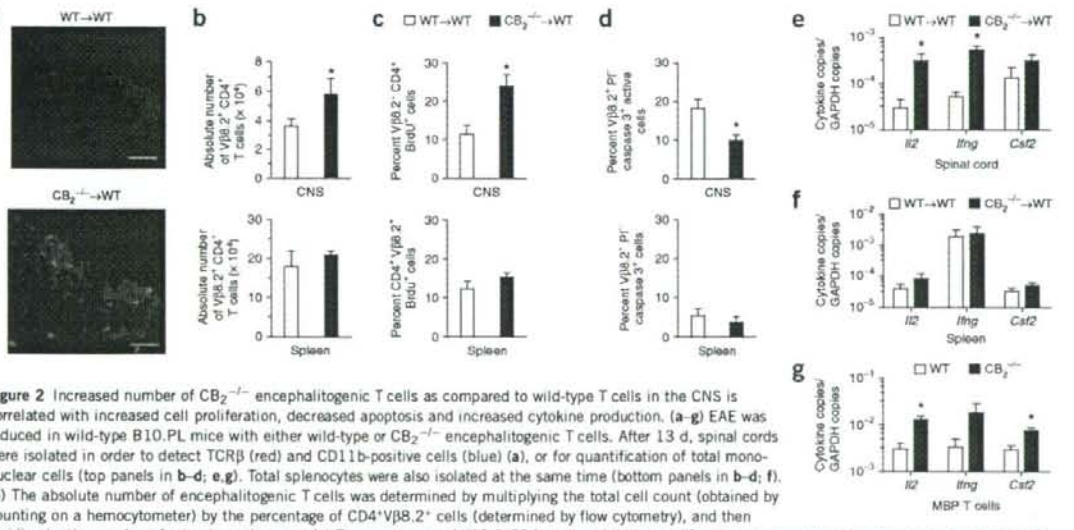

Figure 2 Increased number of $CB_2^{-/-}$ encephalitogenic T cells as compared to wild-type T cells in the CNS is correlated with increased cell proliferation, decreased apoptosis and increased cytokine production. (**a**–**g**) EAE was induced in wild-type B10.PL mice with either wild-type or $CB_2^{-/-}$ encephalitogenic T cells. After 13 d, spinal cords were isolated in order to detect TCRβ (red) and CD11b-positive cells (blue) (**a**), or for quantification of total mononuclear cells (top panels in **b**–**d**; **e**,**g**). Total splenocytes were also isolated at the same time (bottom panels in **b**–**d**; **f**). (**b**) The absolute number of encephalitogenic T cells was determined by multiplying the total cell count (obtained by counting on a hemocytometer) by the percentage of $CD4^+V\beta8.2^+$ cells (determined by flow cytometry), and then dividing by the number of mice in each group. (**c**) The percentage of $V\beta8.2^+CD4^+$ cells exhibiting proliferation, as determined by measuring the percent of $BrdU^+$ cells, is shown. (**d**) The percentage of $V\beta8.2^+$ cells undergoing apoptosis was determined by measuring caspase activity gating on $V\beta8.2^+$propidium iodide $(PI)^-$ cells. In **b**–**d**, error bars represent the mean ± s.d. of three separate experiments, with each individual observation containing pooled cells from five mice. The asterisk indicates a statistically significant change ($P < 0.05$) from the wild-type control group. (**e**–**g**) cDNA was generated from total mononuclear cells (**e**,**f**) or from $V\beta8.2^+CD4^+$ cells (**g**). Expression of *Il2*, *Ifng* and *Csf2* was analyzed by real-time RT-PCR. Quantitative RT-PCR results are presented as a ratio of the number of specific copies to the number of GAPDH copies. The data shown is the average ± s.d. of three separate experiments with each containing pooled RNA from either three or five mice per group. The asterisk indicates a statistically significant increase ($P < 0.05$) from the wild-type control group. Scale bar in **a**, 30 μm.

mRNA was also substantially increased ($P < 0.08$). These data show that the CB_2 receptor plays a role in the function of encephalitogenic T cells, controlling both their survival and cytokine production.

Our cumulative data demonstrate independent roles for the CB_1 and CB_2 receptors in EAE. We found that CB_1 receptors on neurons, but not T cells, mediated suppression by THC, indicating that the stimulation of the CB_1 receptor on lymphocytes is not the mode of action of immunosuppressive cannabinoids *in vivo*. Rather, the CB_2 receptor regulates T-cell effector function in the CNS. Of interest is the specificity of the cannabinoid regulation of CNS T cells. One likely explanation for this finding is that the spleen and plasma contain lower concentrations of endocannabinoids than does CNS tissue[20]. Thus the CB_2 receptor becomes activated once the T cells migrate into the CNS, allowing the CNS to maintain its immunosuppressive microenvironment.

One important implication of these data is that the amount of CB_1 and CB_2 receptor activation is a critical determinant of the severity of EAE. For the CB_1 receptor, administration of an exogenous agonist was required to observe suppression of disease; in contrast, for the CB_2 receptor, a lack of receptor expression on T cells alone was sufficient. This suggests that the endogenous levels of the endocannabinoids are sufficient for CB_2, but not CB_1, receptor agonism. We have previously reported that irradiation reduces spinal cord 2-AG content[21], which would reduce CB_2 receptor agonism. This finding is consistent with $CB_2^{-/-}$ T cells inducing severe EAE in the absence of irradiation. The importance of the CB_2 receptor in T-cell suppression was clearly shown by the finding that irradiation was not required when EAE was induced with $CB_2^{-/-}$ T cells. Similarly, a study using mice deficient in purinergic $P2X_7$ receptors, which have been shown to increase 2-AG production[22], exhibited increased neuronal damage and decreased levels of 2-AG in the brain during EAE (ref. 23). These cumulative data suggest that 2-AG levels play an important role in determining the extent of pathological lesions in EAE.

These studies are in agreement with the premise that cannabinoid receptor agonists would be beneficial for the treatment of multiple sclerosis[9]. The rationale for this is that CB_1 receptor activation could reduce the spasticity associated with multiple sclerosis whereas CB_2 receptor activation could reduce inflammation and, perhaps retard the progression of the disease. Our current data suggest that the T-cell CB_2 receptor is highly activated by its endogenous ligand in the CNS during EAE. We also show a role for the CB_1 receptor on neurons in THC suppression of disease. These data suggest that therapies using cannabinoid agonists will have efficacy in controlling neuronal symptoms of multiple sclerosis, but that a better approach to enhance CB_2 receptor–mediated immune suppression would be to increase endocannabinoid content in the brain or upregulate CB_2 receptor expression on T cells.

METHODS

Mice. Biozzi ABH (H-2^{dq1}) and ABH mice lacking the gene encoding the CB_1 receptor (CB_1) were generated as described[13]. C57BL/6.CB_1^{0f} *loxP*-flanked ('floxed') CB_1 receptor mouse, expressing CB_1 flanked by *loxP* sites[24], was backcrossed with ABH mice for six generations. B6.Cg-Tg(*Nes-cre*)1Kln/J (ref. 25) and B6.Cg-Tg(*Lck-cre*)548Jxm/J (ref. 26) were purchased from Jackson Laboratories and backcrossed to ABH-$CB_1^{-/-}$ for seven generations to produce ABH-$CB_1^{-/-}$-Tg(*Nes-cre*)$^{-/+}$ and ABH-$CB_1^{-/-}$-Tg(*Lck-cre*)$^{-/+}$ mice. These mice express transgenes (Tg) coding for *Cre* recombinase (*Cre*) under the control of either the nestin (*Nes*) or the lymphocyte protein tyrosine kinase (*Lck*) promoters, and result in the Cre-mediated deletion of floxed genes from nerves and some glia and from lymphocytes, respectively. These *Cre* mice were crossed with ABH-CB_1^{0f} mice to produce conditional CB_1 knockout and CB_1-expressing heterozygous littermates, which were used as controls. Observable sedation and significant hypothermia developed within 20 min of injection of 20 mg/kg intraperitoneally (i.p.) of the CB_1 receptor agonist R(+)WIN 55,212-2 (Sigma) in wild-type mice, CB_1 heterozygotes (–5.1 ± 0.1 °C in ABH-$CB_1^{-/f}$-Tg(*Nes-cre*)$^{-/-}$) and conditional T-cell knockouts (–4.5 ± 0.1 °C in ABH-$CB_1^{-/f}$-Tg(*Lck-cre*)$^{-/+}$). This was absent in both whole-body CB_1 receptor knockouts and nerve-conditional CB_1 receptor knockouts (–0.8 ± 0.2 °C in ABH-$CB_1^{-/f}$-Tg(*Nes-cre*)$^{-/+}$), demonstrating functional depletion of the CB_1 receptor from the brain. B10.PL (H-2^{u}) mice were purchased from the Jackson Laboratory or bred locally. Myelin basic protein T-cell receptor (MBP-TCR) transgenic mice have been described[27]. $CB_2^{-/-}$ C57BL/6 mice[28] on the C57BL/6 background were crossed to the MBP-TCR transgenic mice. $CB_1^{-/-}$ C57BL/6 mice used for proliferation experiments were generated by Roche Palo Alto and were backcrossed for eight generations onto the ICR background. The Medical College of Wisconsin Institutional Animal Care and Use Committee approved animal studies at BloodCenter of Wisconsin. Animal studies in the UK were performed under the Animals (Scientific Procedures) Act 1986 and approved by the Home Office of the UK Government.

EAE induction. Adult ABH mice were injected subcutaneously (s.c.) with 1 mg of freeze-dried mouse spinal cord homogenate in Freund's adjuvant on days 0 and 7. Clinical signs were graded as described[13]. THC and CBD were purchased from Sigma or were obtained from the National Institute for Drug Abuse chemical supply program. They were dissolved in dimethyl sulfoxide (DMSO) and PBS (1:1) or in ethanol:cremophor:PBS (1:1:18) before intraperitoneal injection. Mice were typically treated daily from days 10–22 after inoculation. For B10.PL mice, passive EAE induction was performed as described[18]. Active EAE induction was performed as for ABH mice with 400 μg of Ac1-11 myelin basic protein peptide emulsified in complete Freund's adjuvant (CFA) (Chondrex Inc.).

Proliferation and apoptosis assays. Proliferation and apoptosis of CNS mononuclear cells and splenocytes *in vivo* during EAE was measured as described[29]. For proliferation, cells were stained with antibodies specific for CD4 (eBioscience) and Vβ8.2 combined with streptavidin-PE-Cy5 (BD Biosciences) before intracellular staining with a BrdU-specific antibody. For apoptosis, cells were incubated with PhiPhilux-G_2D_2 before staining with a Vβ8.2-specific antibody (BD Biosciences) combined with streptavidin-APC-Cy7 (Biolegend) and a CD4-specific antibody (eBioscience).

Cytokine quantitation. Total RNA was extracted from whole spinal cord or the spleen 13 d after EAE induction as described[18]. Wild-type and $CB_2^{-/-}$ $CD4^+V\beta8.2^+$ T cells were isolated from the CNS of mice 13 d after EAE induction by cell sorting as described[21], and mRNA was isolated using the Dynabeads mRNA DIRECT Micro Kit (Dynal Biotech ASA). *Ifng*, *Il2* and *Csf2* mRNA were quantitated by real-time RT-PCR as described[18]. Sequence specific primers for GAPDH, IFN-γ, and GM-CSF have been described[18,19]. IL-2 primers were as follows: forward, 5′-CCTGAGCAGGATGGAGGATTAGA-3′; reverse, 5′- TCCGAGACATGCCGCAGAC-3′.

Immunohistochemistry. Frozen sections from spinal cords were generated 13 d after EAE induction, as described, and stained with antibodies specific for CD11b (eBioscience) and TCRβ (BD Bioscience)[19].

CB_2 agonist and antagonist treatment of T cells *in vitro*. MBP-specific wild-type and $CB_2^{-/-}$ splenocytes were primed with antigen as for EAE induction for 1 week, at which time 1×10^6 T cells were restimulated with antigen for 24 h in the presence or absence of the CB_2 specific agonist JWH-133 at 200 nM in DMSO. DMSO was added to the controls. Wild-type and $CB_1^{-/-}$ T cells specific for hen egg lysozyme (HEL) were generated by immunizing with 100 μg HEL emulsified in CFA s.c. After 10 d, draining lymph nodes cells were stimulated with 10 μg/ml HEL. After 7 d, the T cells were restimulated with HEL in the presence of JWH-133 as for the MBP-specific T cells with or without 500 nM SR2 or SR1. Following an 18 h incubation, proliferation and cytokine production were measured. JWH-133 is considered a CB_2 receptor agonist because of its high binding affinity (K_i = 3 nM; ref. 30). However, JWH-133 also binds weakly to the CB_1 receptor, at K_i = 680 nM (ref. 30).

Note: Supplementary information is available on the Nature Medicine website.

ACKNOWLEDGMENTS

We thank S. Morris-Islo for assistance with the mice and Roche Palo Alto for providing $CB_1^{-/-}$ mice. This work was supported in part by US National Institutes of Health grants R01 NS046662 (B.N.D.), R01 NS041314 (C.J.H.) and DA09155 (C.J.H.), the BloodCenter Research Foundation (B.N.D.), the Multiple Sclerosis Society of Great Britain and Northern Ireland, the National Multiple Sclerosis Society and Aims2cure. J.L.C. is a Research Fellow of the Japan Society for the Promotion of Science (P03581). The authors thank the National Institute on Drug Abuse chemical supply program for donating chemicals for this study.

AUTHOR CONTRIBUTIONS

K.M. helped design and performed all of the experiments depicted in **Figures 1** and **2** (except **Fig. 1a**) and **Table 2**, with technical advice and assistance from E.D.P., X.C., E.J.C. and M.K.M in B.N.D.'s laboratory. L.P.S. performed the immunohistology in B.N.D.'s laboratory. G.P. bred and screened conditional knockouts and designed and performed EAE experiments. B.L. supervised G.M. in the production of the conditional CB_1 floxed mice, obtained the funding and provided the techniques for screening the mice. J.L.C. performed EAE experiments in T.Y. and D.B.'s laboratories, and performed supportive experiments of cannabinoids in EAE, cytokine analysis and T-cell responses in T.Y.'s laboratory. C.L. produced the generalized CB_1 receptor knockout mouse and provided techniques for their screening. G.G. assisted with intellectual direction and experimental design and obtained funding for the studies and personnel costs. R.G.P. is a cannabinoid pharmacologist who collaborated on the project since its initiation in 1989 providing intellectual input for experimental design, drug selection and obtained compounds for the project. T.Y. obtained funding for the project. N.E.B. provided the $CB_2^{-/-}$ mice. C.J.H. helped with experimental design and writing of the manuscript; her laboratory backcrossed the $CB_1^{-/-}$ mice onto the ICR background. D.B. bred and screened conditional mice, initiated the project and performed and designed EAE experiments (**Fig. 1a** and **Table 1**). B.N.D. supervised K.M. and colleagues and helped with experimental design. D.B. and B.N.D. secured funding and permission to undertake the study and helped write the manuscript.

COMPETING INTERESTS STATEMENT

The authors declare competing financial interests: details accompany the full-text HTML version of the paper at www.nature.com/naturemedicine.

Published online at http://www.nature.com/naturemedicine
Reprints and permissions information is available online at http://npg.nature.com/reprintsandpermissions

1. Hickey, W.F., Hsu, B.L. & Kimura, H. T-lymphocyte entry into the central nervous system. *J. Neurosci. Res.* **28**, 254–260 (1991).
2. Sospedra, M. & Martin, R. Immunology of multiple sclerosis. *Annu. Rev. Immunol.* **23**, 683–747 (2005).
3. Matsuda, L.A., Lolait, S.J., Brownstein, M.J., Young, A.C. & Bonner, T.I. Structure of a cannabinoid receptor and functional expression of the cloned cDNA. *Nature* **346**, 561–564 (1990).
4. Munro, S., Thomas, K.L. & Abu-Shaar, M. Molecular characterization of a peripheral receptor for cannabinoids. *Nature* **365**, 61–65 (1993).
5. Kaminski, N.E., Abood, M.E., Kessler, F.K., Martin, B.R. & Schatz, A.R. Identification of a functionally relevant cannabinoid receptor on mouse spleen cells that is involved in cannabinoid-mediated immune modulation. *Mol. Pharmacol.* **42**, 736–742 (1992).
6. Klein, T.W. *et al.* The cannabinoid system and immune modulation. *J. Leukoc. Biol.* **74**, 486–496 (2003).
7. Van Sickle, M.D. *et al.* Identification and functional characterization of brainstem cannabinoid CB_2 receptors. *Science* **310**, 329–332 (2005).
8. Salzet, M., Breton, C., Bisogno, T. & Di Marzo, V. Comparative biology of the endocannabinoid system possible role in the immune response. *Eur. J. Biochem.* **267**, 4917–4927 (2000).
9. Pertwee, R.G. Cannabinoids and multiple sclerosis. *Pharmacol. Ther.* **95**, 165–174 (2002).
10. Lyman, W.D., Sonett, J.R., Brosnan, C.F., Elkin, R. & Bornstein, M.B. Δ^9-tetrahydrocannabinol: a novel treatment for experimental autoimmune encephalomyelitis. *J. Neuroimmunol.* **23**, 73–81 (1989).
11. Wirguin, I. *et al.* Suppression of experimental autoimmune encephalomyelitis by cannabinoids. *Immunopharmacology* **28**, 209–214 (1994).
12. Arévalo-Martín, A., Vela, J.M., Molina-Holgado, E., Borrell, J. & Guaza, C. Therapeutic action of cannabinoids in a murine model of multiple sclerosis. *J. Neurosci.* **23**, 2511–2516 (2003).
13. Pryce, G. *et al.* Cannabinoids inhibit neurodegeneration in models of multiple sclerosis. *Brain* **126**, 2191–2202 (2003).
14. Rinaldi-Carmona, M. *et al.* SR 144528, the first potent and selective antagonist of the CB2 cannabinoid receptor. *J. Pharmacol. Exp. Ther.* **284**, 644–650 (1998).
15. Rinaldi-Carmona, M. *et al.* SR141716A, a potent and selective antagonist of the brain cannabinoid receptor. *FEBS Lett.* **350**, 240–244 (1994).
16. Do, Y., McKallip, R.J., Nagarkatti, M. & Nagarkatti, P.S. Activation through cannabinoid receptors 1 and 2 on dendritic cells triggers NF-κB-dependent apoptosis: novel role for endogenous and exogenous cannabinoids in immunoregulation. *J. Immunol.* **173**, 2373–2382 (2004).
17. Parolaro, D., Massi, P., Rubino, T. & Monti, E. Endocannabinoids in the immune system and cancer. *Prostaglandins Leukot. Essent. Fatty Acids* **66**, 319–332 (2002).
18. Ponomarev, E.D. *et al.* γδ T cell regulation of IFN-γ production by central nervous system-infiltrating encephalitogenic T cells: correlation with recovery from experimental autoimmune encephalomyelitis. *J. Immunol.* **173**, 1587–1595 (2004).
19. Ponomarev, E.D. *et al.* GM-CSF production by autoreactive T cells is required for the activation of microglial cells and the onset of experimental autoimmune encephalomyelitis. *J. Immunol.* **178**, 39–48 (2007).
20. Sugiura, T. & Waku, K. 2-Arachidonoylglycerol and the cannabinoid receptors. *Chem. Phys. Lipids* **108**, 89–106 (2000).
21. Maresz, K., Carrier, E.J., Ponomarev, E.D., Hillard, C.J. & Dittel, B.N. Modulation of the cannabinoid CB_2 receptor in microglial cells in response to inflammatory stimuli. *J. Neurochem.* **95**, 437–445 (2005).
22. Witting, A., Walter, L., Wacker, J., Moller, T. & Stella, N. P2X$_7$ receptors control 2-arachidonoylglycerol production by microglial cells. *Proc. Natl. Acad. Sci. USA* **101**, 3214–3219 (2004).
23. Witting, A. *et al.* Experimental autoimmune encephalomyelitis disrupts endocannabinoid-mediated neuroprotection. *Proc. Natl. Acad. Sci. USA* **103**, 6362–6367 (2006).
24. Marsicano, G. *et al.* CB1 cannabinoid receptors and on-demand defense against excitotoxicity. *Science* **302**, 84–88 (2003).
25. Tronche, F. *et al.* Disruption of the glucocorticoid receptor gene in the nervous system results in reduced anxiety. *Nat. Genet.* **23**, 99–103 (1999).
26. Hennet, T., Hagen, F.K., Tabak, L.A. & Marth, J.D. T-cell-specific deletion of a polypeptide N-acetylgalactosaminyl-transferase gene by site-directed recombination. *Proc. Natl. Acad. Sci. USA* **92**, 12070–12074 (1995).
27. Dittel, B.N., Merchant, R.M. & Janeway, C.A., Jr Evidence for Fas-dependent and Fas-independent mechanisms in the pathogenesis of experimental autoimmune encephalomyelitis. *J. Immunol.* **162**, 6392–6400 (1999).
28. Buckley, N.E. *et al.* Immunomodulation by cannabinoids is absent in mice deficient for the cannabinoid CB_2 receptor. *Eur. J. Pharmacol.* **396**, 141–149 (2000).
29. Ponomarev, E.D. & Dittel, B.N. γδ T cells regulate the extent and duration of inflammation in the central nervous system by a Fas ligand-dependent mechanism. *J. Immunol.* **174**, 4678–4687 (2005).
30. Huffman, J.W. *et al.* 3-(1',1'-Dimethylbutyl)-1-deoxy-delta8-THC and related compounds: synthesis of selective ligands for the CB_2 receptor. *Bioorg. Med. Chem.* **7**, 2905–2914 (1999).

Published November 17, 2008

JEM

ARTICLE

Aire controls the differentiation program of thymic epithelial cells in the medulla for the establishment of self-tolerance

Masashi Yano,[1] Noriyuki Kuroda,[1] Hongwei Han,[1] Makiko Meguro-Horike,[1] Yumiko Nishikawa,[1] Hiroshi Kiyonari,[2] Kentaro Maemura,[3] Yuchio Yanagawa,[4] Kunihiko Obata,[5] Satoru Takahashi,[6] Tomokatsu Ikawa,[7] Rumi Satoh,[7] Hiroshi Kawamoto,[7] Yasuhiro Mouri,[1] and Mitsuru Matsumoto[1]

[1]Division of Molecular Immunology, Institute for Enzyme Research, University of Tokushima, Tokushima 770-8503, Japan
[2]Laboratory for Animal Resources and Genetic Engineering, Center for Developmental Biology, Institute of Physical and Chemical Research (RIKEN) Kobe, Kobe 650-0047, Japan
[3]Department of Anatomy and Cell Biology, Division of Basic Medicine I, Osaka Medical College, Osaka, 569-8686, Japan
[4]Department of Genetic and Behavioral Neuroscience, Gunma University Graduate School of Medicine, Maebashi 371-8511, Japan
[5]Neuronal Circuit Mechanisms Research Group, RIKEN Brain Science Institute, Saitama 351-0198, Japan
[6]Institute of Basic Medical Sciences and Laboratory Animal Resource Center, Center for Tsukuba Advanced Research Alliance, University of Tsukuba, Tsukuba 305-8575, Japan
[7]Laboratory for Lymphocyte Development, RIKEN Research Center for Allergy and Immunology, Kanagawa 230-0045, Japan

The roles of autoimmune regulator (Aire) in the expression of the diverse arrays of tissue-restricted antigen (TRA) genes from thymic epithelial cells in the medulla (medullary thymic epithelial cells [mTECs]) and in organization of the thymic microenvironment are enigmatic. We approached this issue by creating a mouse strain in which the coding sequence of green fluorescent protein (GFP) was inserted into the *Aire* locus in a manner allowing concomitant disruption of functional Aire protein expression. We found that Aire$^+$ (i.e., GFP$^+$) mTECs were the major cell types responsible for the expression of Aire-dependent TRA genes such as *insulin 2* and *salivary protein 1*, whereas Aire-independent TRA genes such as *C-reactive protein* and *glutamate decarboxylase 67* were expressed from both Aire$^+$ and Aire$^-$ mTECs. Remarkably, absence of Aire from mTECs caused morphological changes together with altered distribution of mTECs committed to Aire expression. Furthermore, we found that the numbers of mTECs that express involucrin, a marker for terminal epidermal differentiation, were reduced in Aire-deficient mouse thymus, which was associated with nearly an absence of Hassall's corpuscle-like structures in the medulla. Our results suggest that Aire controls the differentiation program of mTECs, thereby organizing the global mTEC integrity that enables TRA expression from terminally differentiated mTECs in the thymic microenvironment.

CORRESPONDENCE
Mitsuru Matsumoto:
mitsuru@ier.tokushima-u.ac.jp

Abbreviations used: Ab, antibody; Ag, antigen; Aire, autoimmune regulator; APECED, autoimmune-polyendocrinopathy-candidiasis ectodermal dystrophy; CRP, C-reactive protein; EpCAM, epithelial cell adhesion molecule 1; FSC, forward scatter; GAD67, glutamate decarboxylase 67; K5, keratin 5; mTEC, medullary thymic epithelial cell; SAP1, salivary protein 1; SSC, side scatter; TRA, tissue-restricted Ag; UEA-1, *Ulex europaeus* agglutinin 1.

Autoimmune diseases are mediated by sustained adaptive immune responses specific for self-antigens (Ags) through unknown pathogenic mechanisms. Although breakdown of self-tolerance is considered to be the key event in the disease process, the mechanisms that allow the production of autoantibodies and/or autoreactive lymphocytes are largely enigmatic (1). Autoimmune-polyendocrinopathy-candidiasis ectodermal dystrophy (APECED; OMIM 240300) is a rather rare autoimmune disease affecting mainly the endocrine glands. Because mutation of a single gene, *autoimmune regulator* (*AIRE*), is solely responsible for the development of APECED, understanding the relationship between *AIRE* gene malfunction and the breakdown of self-tolerance promises to help unravel

The online version of this article contains supplemental material.

The Rockefeller University Press $30.00
J. Exp. Med. Vol. 205 No. 12 2827-2838
www.jem.org/cgi/doi/10.1084/jem.20080046

the pathogenesis of not only APECED but also other types of autoimmune diseases (2, 3).

One of the most important aspects of AIRE in the context of autoimmunity is its limited tissue expression in medullary thymic epithelial cells (mTEC) (4, 5). mTECs are believed to play major roles in the establishment of self-tolerance by eliminating autoreactive T cells (negative selection) and/or by producing immunoregulatory T cells, which together prevent $CD4^+$ T cell–mediated organ-specific autoimmune diseases (6, 7). For this purpose, mTECs appear to express a set of self-Ags encompassing many or most of the self-Ags expressed by parenchymal organs. Supporting this hypothesis, analysis of gene expression in the thymic stroma has demonstrated that mTECs are a specialized cell type in which promiscuous expression of a broad range of peripheral tissue-restricted Ag (TRA) genes (i.e., promiscuous gene expression) is an autonomous property (8). Aire in mTECs has been suggested to regulate this promiscuous gene expression (9–11) through as yet undetermined mechanisms.

From a mechanistic viewpoint, there are two possible models to explain the function of Aire in the thymic organogenesis required for the establishment of self-tolerance. First, Aire may play a tolerogenic role within the types of mTECs characterized by Aire expression. In other words, the presence of Aire within cells is necessary in order for them to function normally as tolerance-establishing cells. Consistent with this idea, the current prevailing view on the roles of Aire in establishing self-tolerance is that Aire-positive cells are the major cell types that show promiscuous gene expression and that the lack of Aire protein within cells impairs their tolerogenic function because of the reduced transcription of TRA genes, although the developmental process of mTECs is otherwise unaltered in the absence of Aire (model 1). The second model hypothesizes that Aire is necessary for the developmental program of mTECs, including Aire-positive cells themselves. In this case, we assume that what are called Aire-positive mTECs and other Aire-dependent cell-types do not develop normally in the absence of Aire. Given that acquisition of the properties of promiscuous gene expression depends on the maturation status of mTECs (see Results and Discussion), impaired promiscuous gene expression from Aire-deficient mice can be associated with a defect of such an Aire-dependent developmental program in mTECs (model 2). Although it is still controversial whether reduced transcription of particular TRA genes in Aire-deficient mTECs can account for the development of autoimmunity targeting the corresponding self-Ags in Aire-deficient mice by itself (11–15), it is critical to determine which model provides a more appropriate explanation of Aire-dependent promiscuous gene expression to further elucidate the molecular aspects of Aire (16). Model 1 would direct research toward the mechanisms underlying how a single *Aire* gene can regulate a large number of target genes (i.e., TRA genes), whereas model 2 would accelerate studies of the developmental program of mTECs in which Aire plays a pivotal role. These two models can be tested if we can monitor the developmental process of mTECs committed to Aire expression in both the presence and absence of functional Aire protein.

This issue regarding the roles of Aire in thymic organogenesis is also directly linked to the fundamental question of how mTECs acquire their unique ability to express a broad range of self-Ags (i.e., promiscuous gene expression). The terminal differentiation model assumes that mTECs eventually acquire the capacity for promiscuous gene expression by becoming differentiated, more mature, and more promiscuous (7, 10). This model suggests that mTECs, especially Aire-positive cells, are specialized cell types that have acquired this ability through differentiation. In this context, it is noteworthy that the transcriptional machinery necessary for promiscuous gene expression other than Aire protein is considered to be acquired by mTECs independent of Aire expression in this model. The model suggests that the transcriptional unit for promiscuous gene expression becomes fully active when Aire starts to be expressed in terminally differentiated mTECs. In contrast, the developmental model considers that promiscuous gene expression is a reflection of the multipotency of immature mTECs before the developmental fate of particular cell types is determined (17). In this model, expression of a broad spectrum of TRA genes is regulated by conserved developmental programs that are active in developing mTECs, and Aire and/or $Aire^+$ cells control this process (18). Accordingly, the developmental model considers that Aire acts at the early developmental stage of mTEC differentiation, which is in marked contrast to the timing of Aire expression proposed in the terminal differentiation model. Thus, the terminal differentiation model and the developmental model favor models 1 and 2, respectively, proposed for the roles of Aire in promiscuous gene expression and self-tolerance (19).

To investigate in more detail the roles of Aire in thymic organogenesis, we have used a knock-in mouse strategy in which the coding sequence of GFP was inserted into the *Aire* gene locus in a manner allowing concomitant disruption of functional Aire protein expression. This strategy allowed us to distinguish mTECs committed to expressing Aire from Aire-nonexpressing mTECs, in both the presence and absence of functional Aire protein. In addition, with the use of knock-in mice in which thymic TRA (i.e., *glutamate decarboxylase 67* [*GAD67*]) expression can be monitored by GFP expression we also examined the cell types of mTECs responsible for promiscuous gene expression in situ. The results suggest that Aire promotes the differentiation program of mTECs and that promiscuous gene expression is accomplished in terminally differentiated mTECs that have fully matured in the presence of Aire protein.

RESULTS

Establishment of Aire/GFP knock-in mice

To examine the molecular and cellular contribution of Aire to thymic organogenesis, we established Aire/GFP knock-in mice in which expression of the GFP gene is under the transcriptional control of the endogenous *Aire* gene. In this strategy, modification of the *Aire* gene locus was minimized by inserting a GFP-neomycin resistance (neo^r) gene cassette (gfp-neo) (20) between exon 1 and exon 2 (Fig. 1 A). After

Published November 17, 2008

establishing *Aire*$^{+/gfp\text{-}neo}$ mice, they were crossed with a general deleter Cre recombinase-expressing transgenic line (21) to remove the neo^r gene cassette, which contains the herpes simplex virus *thymidine kinase* gene promoter for efficient neo^r gene expression. After confirming the removal of the neo^r gene cassette (Fig. 1 B), mice were crossed with C57BL/6 mice to select a line containing the GFP knock-in allele but not the Cre recombinase-expressing transgenic allele. *Aire*$^{+/gfp}$ mice were then crossed to obtain *Aire*$^{gfp/gfp}$ mice, which have a null mutation for the *Aire* gene because of disruption of the *Aire* gene by insertion of the GFP gene (Fig. 1 B). As expected, *Aire*$^{gfp/gfp}$ mice, but not *Aire*$^{+/gfp}$ mice, showed no expression of endogenous Aire in the thymus, as detected with polyclonal anti-Aire antibody (Ab) recognizing peptides located within the proline-rich region of Aire (unpublished data).

Using immunohistochemistry, we first examined whether GFP expression from *Aire*$^{+/gfp}$ mouse thymus reflects endogenous *Aire* gene expression. Stromal cells showing variable extents of GFP expression in the cytoplasm and nucleus were scattered throughout the thymic medulla (Fig. 1 C). The medullary region was identified by staining with *Ulex europaeus* agglutinin 1 (UEA-1) (Fig. 2 A), anti–epithelial cell adhesion molecule 1 (EpCAM) mAb (Fig. 2 B), or anti–keratin 5 (K5) Ab (Fig. S1 A, available at http://www.jem.org/cgi/content/full/jem.20080046/DC1). GFP-expressing cells from *Aire*$^{+/gfp}$ mouse thymus showed a dendritic to fibroblastic morphology and were enriched at the cortico-medullary junction (Fig. 1 C; Fig. 2, A and B; and Fig. S1 A). When doubly stained with anti-Aire Ab, most of the GFP-expressing cells contained variable amounts of Aire nuclear dots within their nuclei (Fig. 1 C), indicating that GFP expression is under the transcriptional control of the authentic *Aire* gene. However, a few cells showed Aire nuclear dots without any detectable GFP expression (Fig. 1 C, arrows) or expressed GFP without obvious Aire nuclear dots (not depicted). As expected, *Aire*$^{+/+}$ mouse thymus showed no GFP signals (Fig. 2, A and B). Notably, most of the CD11c-positive DCs in the thymus were GFP negative (Fig. S1 B), suggesting that Aire expression from thymic DCs is negligible compared with that from mTECs.

Altered thymic organization in Aire-deficient mice

We then examined the effect of Aire deficiency on thymic organization in *Aire*$^{gfp/gfp}$ mouse thymus sections, focusing on the production of cells genetically marked with GFP and, therefore, active in *Aire* gene transcription but lacking functional Aire protein. There were many GFP$^+$ "Aire-less" TECs within the medulla (Figs. 2, A and B; and Fig. S1 A), indicating clearly that Aire protein itself is not necessary for the production of particular mTEC lineages committed to express Aire. However, detailed inspection demonstrated that the morphology and location of GFP$^+$ cells from *Aire*$^{gfp/gfp}$ thymus were altered compared with those of GFP$^+$ cells containing functional Aire protein from *Aire*$^{+/gfp}$ mouse thymus. First, we noticed that the cell shape of GFP$^+$ mTECs lacking functional Aire protein was altered; in *Aire*$^{gfp/gfp}$ thymus, more GFP$^+$ cells exhibited a globular shape instead of a dendritic to fibroblastic morphology, compared with *Aire*$^{+/gfp}$ thymus (Fig. 2 C, arrows). The lower preponderance of a dendritic shape of GFP$^+$ Aire-less mTECs was verified by statistical analysis. We calculated the level of cell shape complexity for each GFP$^+$ cell by dividing the length of the cellular periphery by the cell area using a computer program (i.e., the higher

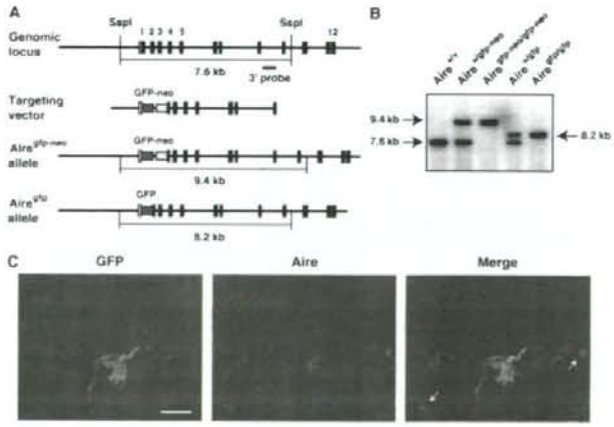

Figure 1. Establishment of Aire/GFP knock-in mice. (A) Targeted insertion of the GFP gene into the *Aire* gene locus by homologous recombination. SspI, *SspI* restriction site. (B) Southern blot analysis of genomic DNA from offspring of Aire/GFP knock-in mice. Tail DNA was digested with *SspI* and hybridized with the 3′ probe shown in A. (C) Concomitant expression of GFP (green) and endogenous mouse Aire (red) assessed by immunohistochemistry of a thymus section from an *Aire*$^{+/gfp}$ mouse. Cells positive for Aire staining but negative for GFP expression are marked with arrows. Bar, 20 μm. One representative experiment from a total of four repeats is shown.

the value, the more complex the cell shape). GFP$^+$ cells from *Aire*$^{gfp/gfp}$ thymus showed lower values (i.e., less complexity per cell) and a narrower distribution of values (i.e., less heterogeneity of cell shape) than those from *Aire*$^{+/gfp}$ thymus (Fig. 2 D). Because a gene-dosage effect has been noticed at the *Aire* gene locus (11), we carefully excluded the possibility that the altered shape of GFP$^+$ cells from *Aire*$^{gfp/gfp}$ thymus was due simply to higher GFP protein expression within each cell, i.e., imposing a potentially toxic burden on the cells. For this purpose, we crossed *Aire*$^{+/gfp}$ mice with *Aire*$^{-/-}$ mice (12) to establish *Aire*$^{-/gfp}$ mice in which the *gfp* allele is single, as in *Aire*$^{+/gfp}$ mice (Fig. S2 A). Similarly to the *Aire*$^{gfp/gfp}$ thymus analysis, GFP$^+$ cells from *Aire*$^{-/gfp}$ thymus demonstrated less complexity of cell shape than those from *Aire*$^{+/gfp}$ thymus, as confirmed using the same method of statistical analysis (Fig. S2 B).

Although we analyzed the thymic organization of *Aire*$^{gfp/gfp}$ mice before the onset of autoimmune pathology (i.e., 4–6 wk after birth), we also excluded the possibility that the altered cell shape of GFP$^+$ cells from *Aire*$^{gfp/gfp}$ thymus was secondary to the autoimmune phenotypes by establishing *Aire*$^{-/gfp}$ mice expressing the OT-II TCR transgene in which the autoreactive T cell repertoire is absent (Fig. S3 A). Morphological changes in GFP$^+$ cells were similarly observed in these mice (Fig. S3 B), suggesting that the altered shape of GFP$^+$ cells lacking Aire protein was independent of autoimmune phenotype.

Second, we noticed that the distribution pattern of mTECs committed to Aire expression was also affected in the absence of functional Aire protein. In contrast with the enrichment of GFP$^+$ cells from *Aire*$^{+/gfp}$ thymus at the cortico-medullary junction, GFP$^+$ cells from *Aire*$^{gfp/gfp}$ thymus tended to be localized

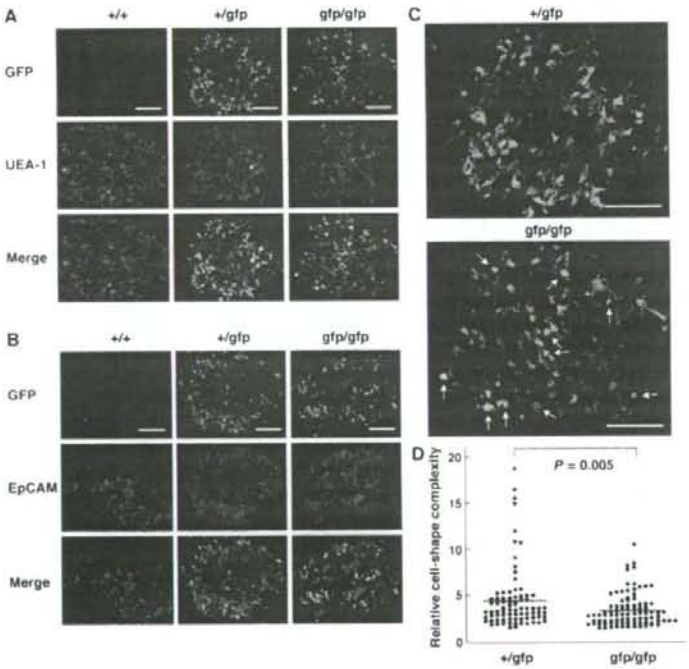

Figure 2. Altered morphology and distribution of mTECs committed to express Aire in the absence of functional Aire protein.
(A and B) mTECs active in *Aire* gene transcription were visualized by immunohistochemistry with anti-GFP Ab (green). The medullary region was identified by staining with UEA-1 (A) or anti-EpCAM mAb (B; red). Bars, 100 µm. One representative experiment from a total of five repeats is shown. (C) Enlargement of the staining with anti-GFP Ab from A for demonstration of altered morphology and distribution of mTECs committed to express Aire in *Aire*$^{gfp/gfp}$ mouse thymus. There were more GFP$^+$ cells with globular shapes (bottom, arrows) in *Aire*$^{gfp/gfp}$ thymus than in *Aire*$^{+/gfp}$ thymus. GFP$^+$ cells from *Aire*$^{-/gfp}$ thymus were enriched at the cortico-medullary junction (top), whereas GFP$^+$ cells from *Aire*$^{gfp/gfp}$ thymus tended to be localized more evenly within each medulla or even enriched at the center of the medulla (bottom). Bars, 100 µm. One representative experiment from a total of five repeats is shown. (D) Morphological changes in the shape of GFP$^+$ cells from *Aire*$^{gfp/gfp}$ mouse thymus demonstrated in C were analyzed statistically. Each circle corresponds to the relative cell shape complexity of a single GFP$^+$ cell calculated with a computer program (see Materials and methods). A total of 80 and 88 GFP$^+$ cells from *Aire*$^{+/gfp}$ and *Aire*$^{gfp/gfp}$ thymi, respectively, were evaluated. Red lines represent mean values. Two mice for each group were analyzed, and similar results were obtained from a total of three repeats.

Published November 17, 2008

more uniformly within each medulla or even enriched at the medulla center (Fig. 2 C and Fig. S1 A). Altered distribution of GFP$^+$ Aire-less mTECs was also evident in *Aire*$^{-/cb}$ mice (Fig. S2 A), as well as in *Aire*$^{-/cb}$ mice expressing the nonautoreactive OT-II TCR transgene (Fig. S3 A). Collectively, production of a particular mTEC lineage committed to express Aire is not determined by Aire protein alone. However, Aire deficiency in these cells results in morphological changes together with altered location within the medulla, suggesting a role of Aire in the differentiation program of mTECs in a cell-intrinsic manner.

Analysis of embryonic thymus demonstrated that GFP$^+$ cells were absent at embryonic day 13.5, but clearly present at embryonic day 16.5 in both *Aire*$^{+/cb}$ and *Aire*$^{cb/cb}$ mice (Fig. S1 C). Although the effect of absence of Aire protein on the location of GFP$^+$ cells from *Aire*$^{cb/cb}$ mice at the embryonic and early P1 (postneonatal) stages was difficult to evaluate because of the less organized thymic structure together with relatively small numbers of GFP$^+$ cells at those stages, morphological alteration of each mTEC committed to Aire expression was already evident at the neonatal stage (P1; Fig. S4 A), as confirmed by the same statistical analysis applied to Fig. 2 D (Fig. S4 B). The properties of GFP$^-$ (i.e., Aire nonexpressing) mTECs as evaluated by immunohistochemistry with UEA-1, anti-EpCAM Ab (Fig. 2, A and B), anti-K5 Ab (Fig. S1 A), ER-TR5 Ab, anti–claudin 3/4 Abs, and MTS10 Ab (not depicted) showed no obvious difference between *Aire*$^{+/cb}$ and *Aire*$^{cb/cb}$ adult thymi.

In addition to the histological evaluation of mTECs based on Aire/GFP expression, another possibility that Aire controls the differentiation program of mTECs has emerged from studies focusing on the cell differentiation markers expressed by mTECs. In the skin, involucrin expression is restricted to postmitotic epithelial cells and serves as a marker of epidermal and follicular terminal differentiation (22). Interestingly, immunohistochemistry of the human thymus using anti-involucrin Ab stains characteristic swirled epithelial structures known as Hassall's corpuscles (23), which is consistent with the fact that Hassall's corpuscles are composed of terminally differentiated mTECs (24). When thymus sections from Aire-sufficient mice were stained with anti-involucrin Ab, involucrin-expressing cells were scattered within the EpCAM$^+$ thymic medulla (Fig. 3 A). The number of involucrin-expressing cells was age dependent and declined between 8 and 11 wk (Fig. 3 B and Table S1, available at http://www.jem.org/cgi/content/full/jem.20080046/DC1). In addition, we occasionally found larger involucrin-expressing structures with a hyalinized degenerated core in the thymic medulla from Aire-sufficient mice, which is reminiscent of Hassall's corpuscles in human thymus (Fig. 3 C). Remarkably, the numbers of mTECs expressing involucrin in Aire-deficient mice were significantly lower than those in Aire-sufficient mice, especially at 4 and 8 wk of age (Fig. 3 B). Furthermore, we observed no typical Hassall's corpuscle-like structures in the thymus of Aire-deficient mice at any age, which is in contrast to those seen in Aire-sufficient mice (Table S1). These results further support the notion that lack of Aire in mTECs alters their differentiation program, thereby altering mTEC integrity.

Next, we used flow cytometric analysis to examine GFP-expressing cells from the thymus. Thymic stromal cells were released enzymatically from adult thymi and stained with anti-CD45 mAb and UEA-1, together with anti-CD80 and anti–MHC class II mAbs. *Aire*$^{+/cb}$ thymus contained 4.5% UEA-1$^+$GFP$^+$ (i.e., Aire$^+$) cells (from here on simply designated GFP$^+$ cells) in the population of CD45$^-$ stromal cells (Fig. 4 A). When forward scatter (FSC) and side scatter (SSC) parameters were compared between GFP$^+$ cells and UEA-1$^+$GFP$^-$ cells (from here on simply designated GFP$^-$ cells), GFP$^+$ cells were larger and more broadly distributed compared with GFP$^-$ cells (Fig. 4 B, left), suggesting a distinct cellular morphology of Aire$^+$ cells among mTECs. *Aire*$^{cb/cb}$ thymus also contained GFP$^+$ cells in the population of CD45$^-$ stromal cells (Fig. 4 A), as already observed by immunohistochemical analysis (Figs. 2 and S1). Interestingly, the proportion of GFP$^+$ cells in *Aire*$^{cb/cb}$ thymus was consistently

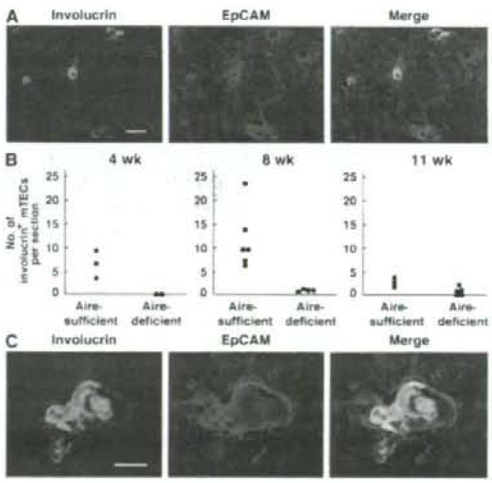

Figure 3. Reduced numbers of terminally differentiated mTECs in the absence of Aire. (A) Involucrin-expressing mTECs (green) were scattered within the thymic medulla (red; stained with anti-EpCAM Ab) of Aire-sufficient mice. Bar, 50 µm. (B) Numbers of involucrin-expressing mTECs were reduced in Aire-deficient mice at 4 (left) and 8 (middle) wk of age. Numbers of involucrin-expressing mTECs in Aire-sufficient mice declined at 11 wk of age (right). Each circle corresponds to the mean number of involucrin-expressing mTECs per section examined in individual mice. Detailed information for the mice examined from a total of five experiments is presented in Table S1 (available at http://www.jem.org/cgi/content/full/jem.20080046/DC1). (C) Hassall's corpuscle-like structures seen in Aire-sufficient mouse thymus stained with anti-involucrin Ab (green) together with anti-EpCAM Ab (red). These discrete and larger involucrin-expressing structures were scarcely detectable in Aire-deficient mouse thymus. Bar, 20 µm. One representative experiment from a total of five repeats is shown.

Published November 17, 2008

30–40% higher than in *Aire*$^{+/gfp}$ thymus (Fig. 4 A). Consequently, the ratio of GFP$^+$ cells to GFP$^-$ cells was higher in *Aire*$^{gfp/gfp}$ thymus (~1:5) compared with that in *Aire*$^{+/gfp}$ thymus (~1:10). Although the difference in FSC/SSC parameters between GFP$^+$ and GFP$^-$ cells observed for *Aire*$^{+/gfp}$ mice was also seen in *Aire*$^{gfp/gfp}$ mice (Fig. 4 B, right), FSC/SSC plots of GFP$^+$ cells from *Aire*$^{gfp/gfp}$ mice showed a more condensed profile over a narrower region compared with GFP$^+$ cells from *Aire*$^{+/gfp}$ mice (Fig. 4 B, top), which might reflect the morphological changes in GFP$^+$ mTECs observed by immunohistochemistry (Fig. 2 C). We recorded no GFP expression from CD45$^+$ hematopoietic cells (not depicted) or from CD45$^-$UEA-1$^-$ thymic stromal cells from either *Aire*$^{+/gfp}$ or *Aire*$^{gfp/gfp}$ mice (Fig. 4 A).

We then analyzed the expression of CD80 and MHC class II from each of the populations separated on the basis of GFP expression and UEA-1 binding. GFP$^+$ cells from *Aire*$^{+/gfp}$ mice expressed both CD80 and MHC class II at high levels (CD80^{hi}/class II^{hi}), whereas GFP$^-$ cells from the same animals expressed intermediate to low levels of both CD80 and MHC class II (Fig. 4 C, left). GFP$^+$ cells from *Aire*$^{gfp/gfp}$ thymus were also CD80^{hi}/class II^{hi} (Fig. 4 C, right), indicating that expression of these Ag presentation-related molecules was Aire independent. Indeed, expression levels of both CD80 and MHC class II from GFP$^+$ cells were almost indistinguishable between *Aire*$^{+/gfp}$ and *Aire*$^{gfp/gfp}$ mice when the two flow cytometric profiles were merged (Fig. 4 D, left). However, although difference was small, expression of both CD80 and MHC class II from GFP$^-$ cells from *Aire*$^{gfp/gfp}$ mice was consistently lower than that from *Aire*$^{+/gfp}$ mice (Fig. 4 D, right). This result may indicate that the absence of normal Aire-expressing cells from the medulla is accompanied by phenotypic alteration of Aire-nonexpressing mTECs, which was not evident with the immunohistochemical analysis with the commonly used medullary epithelial cell markers (Fig. 2, A and B; and Fig. S1 A). Collectively, the results suggest that *Aire* deficiency results in a global alteration of the thymic microenvironment that involves not only mTECs committed to express Aire but also the Aire-nonexpressing mTECs that surround Aire$^+$ cells.

Aire-dependent TRA gene expression

Although Aire has been suggested to regulate promiscuous gene expression in mTECs (9, 10), demonstration that Aire$^+$ cells are the major source of promiscuous gene expression from mTECs is still incomplete in the absence of appropriate cell markers for Aire-expressing cell lineages. Existing data for promiscuous gene expression from mTECs were obtained

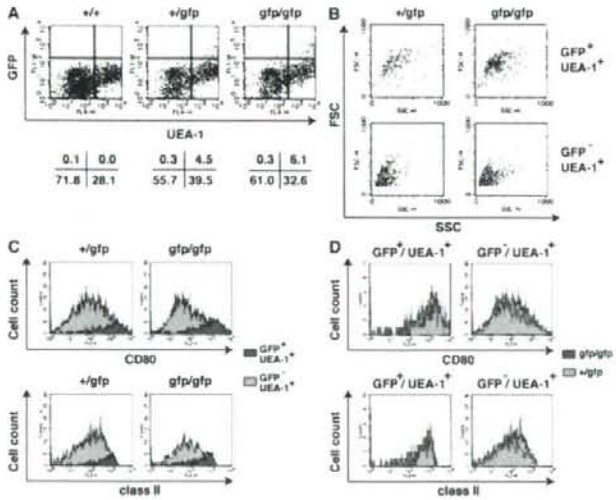

Figure 4. Global alteration of mTEC phenotypes in the absence of Aire. (A) Detection of GFP-expressing cells from thymic stroma by flow cytometric analysis. CD45$^-$ thymic stromal cells were analyzed for the expression of GFP together with binding of UEA-1. Percentages of cells from each fraction are indicated below. (B) mTECs committed to express Aire were larger than mTECs noncommitted to express Aire, irrespective of the presence of Aire protein. FSC/SSC profiles of mTECs committed to express Aire were altered in the absence of functional Aire protein (top). Each FSC/SSC profile was obtained by back gating the corresponding fractions from A based on the expression of GFP and UEA-1. (C) CD80 and MHC class II expression levels were higher in mTECs committed to express Aire than in mTECs noncommitted to express Aire, irrespective of the presence of functional Aire protein. Filled profiles in green and gray are from GFP$^+$ and GFP$^-$ mTECs, respectively. (D) CD80 and MHC class II expression from mTECs committed to express Aire were indistinguishable between *Aire*$^{+/gfp}$ and *Aire*$^{gfp/gfp}$ mice (left) but were reduced in mTECs noncommitted to express Aire in the absence of functional Aire protein (right). Filled profiles in gray and green lines are from *Aire*$^{+/gfp}$ and *Aire*$^{gfp/gfp}$ mice, respectively. Flow cytometric profiles from C were merged for comparison. One representative result from a total of more than five repeats is shown.

Published November 17, 2008

by flow cytometric sorting using surrogate Aire$^+$ cell markers such as CD80 and MHC class II. As a result, it is not yet clear which population of mTECs (i.e., Aire-expressing or Aire-nonexpressing mTECs) is deficient in promiscuous gene expression as a result of absence of functional Aire protein. To answer this question, we separated GFP$^+$ and GFP$^-$ mTECs from both *Aire*$^{+/gfp}$ and *Aire*$^{gfp/gfp}$ mice and examined the expression of several TRA genes, including both Aire-dependent (i.e., *insulin 2* and *salivary protein 1* [*SAP1*]) and Aire-independent (*C-reactive protein* [*CRP*]) TRA genes; expression of the former and the latter gene classes has been demonstrated to be reduced or unchanged, respectively, in CD80^{hi}/class II^{hi} Aire-deficient mTECs (9, 10). GFP$^+$ mTECs from *Aire*$^{+/gfp}$ mice showed the highest expression of *insulin 2* and *SAP1*, and expression of those genes was much lower in GFP$^-$ mTECs from the same animals (Fig. 5). Remarkably, both GFP$^+$ and GFP$^-$ mTECs from *Aire*$^{gfp/gfp}$ mice expressed almost none of the Aire-dependent TRA genes *insulin 2* and *SAP1*. mTECs defined by UEA-1 binding from *Aire*$^{+/+}$ mice, which includes both Aire$^+$ and Aire$^-$ cells, showed intermediate expression of those genes. These results clearly indicate two important features of promiscuous gene expression in mTECs. First, Aire$^+$ mTECs are the major cell types responsible for the expression of Aire-dependent TRA genes. Second, mTECs cannot express Aire-dependent TRA genes in the absence of functional Aire protein, even though the lineage commitment to express Aire and the expression of Ag presentation-related molecules, such as CD80 and MHC class II, are preserved (Fig. 4 C). It is important to emphasize that the latter observation does not necessarily mean that Aire acts on the already existing transcriptional machinery required for TRA gene expression within established terminally differentiated mTECs. Rather, in the light of the fact that GFP$^+$ Aire-less mTECs show defective development, as indicated by their altered morphology and distribution, we suggest that Aire$^+$ mTECs acquire their unique machinery for promiscuous gene expression only when they have fully achieved maturation with the help of Aire protein (see Discussion and see Fig. 8).

In marked contrast to Aire-dependent TRA genes, expression of an Aire-independent TRA gene, *CRP*, from GFP$^+$ mTECs was indistinguishable between *Aire*$^{+/gfp}$ and *Aire*$^{gfp/gfp}$ mice. *CRP* expression from GFP$^-$ mTECs was detectable, although the levels were lower than from GFP$^+$ mTECs, and was also similar between *Aire*$^{+/gfp}$ and *Aire*$^{gfp/gfp}$ mice (Fig. 5). As expected, the *Aire* gene was highly expressed from GFP$^+$ mTECs of *Aire*$^{+/gfp}$ mice, although a low level of *Aire* gene expression was detected from GFP$^-$ mTECs, which is possibly a result of slight contamination by cells expressing a trace amount of GFP (i.e., Aire) in this fraction. Expression of the *Aire* gene from both GFP$^+$ and GFP$^-$ cells of *Aire*$^{gfp/gfp}$ mice was at background levels.

Aire-independent TRA gene expression in situ from mTECs

The results in the previous section suggest that individual mTECs do not express a broad array of TRA genes. Rather, each mTEC seems to express a different spectrum of TRA genes. Some TRA genes, such as *insulin 2* and *SAP1* (previously recognized as Aire-dependent genes; references 9, 10), were predominantly expressed from cells of the Aire$^+$ mTEC lineage only when Aire protein was present within the cells, and other TRA genes, such as *CRP* (previously recognized as an Aire-independent gene; references 9, 10), were expressed from both Aire$^+$ and Aire$^-$ mTECs irrespective of the presence of Aire protein. The latter situation was further investigated with the use of GAD67/GFP knock-in mice (*GAD67*$^{+/gfp}$ mice). *GAD67*, an Aire-independent TRA gene that is expressed in the brain and pancreas, is

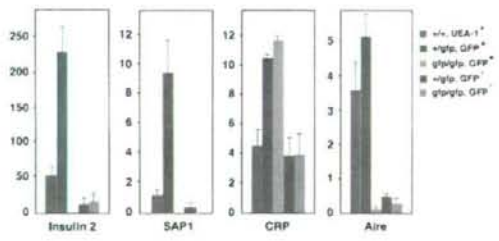

Figure 5. TRA gene expression from mTECs assessed by real-time PCR. Expression of *insulin 2*, *SAP1*, *CRP*, and *Aire* was examined from each fraction of mTECs sorted on the basis of the flow cytometric profile demonstrated in Fig. 4 A. Color bars corresponding to each fraction are indicated on the right. Aire$^+$ mTECs were the major cell types responsible for the expression of Aire-dependent TRA genes (*insulin 2* and *SAP1*), whereas an Aire-independent TRA gene (*CRP*) was expressed from both Aire$^+$ and Aire$^-$ mTECs. Aire expression was assessed to verify the proper sorting of each mTEC fraction. Numbers are relative gene expression level compared with that of the *Hprt* gene. Results are expressed as the mean ± SEM for triplicate wells of one representative experiment from a total of three repeat experiments.

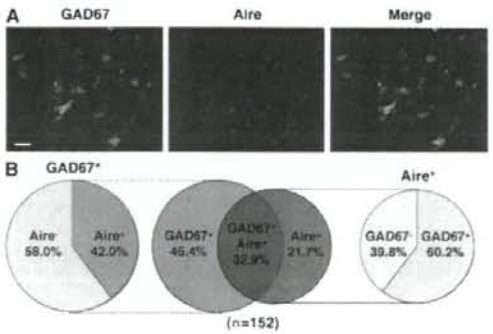

Figure 6. Expression of the Aire-independent TRA gene *GAD67* and of Aire from mTECs in situ. (A) Expression of the *GAD67* gene and Aire was detected by immunohistochemistry with anti-GFP Ab (green) and anti-Aire Ab (red), respectively, in thymus sections from GAD67/GFP knock-in mice. Bar, 20 µm. (B) Results obtained as described for A were calculated for a total of 152 mTECs expressing the *GAD67* gene and/or Aire. One representative experiment from a total of three repeats is shown.

also active in mTECs from *GAD67*$^{+/gfp}$ mice (25). Using immunohistochemistry, we examined the expression of GAD67 together with Aire in *GAD67*$^{+/gfp}$ mouse thymus sections. There were three types of TECs: GAD67^{+}Aire^{-} (45.4%), GAD67^{+}Aire^{+} (32.9%), and GAD67^{-}Aire^{+} (21.7%) (Fig. 6, A and B). Among the GAD67^{+} mTECs, 42.0% expressed Aire and the rest did not (Fig. 6 B), consistent with the Aire-independent nature of *GAD67* gene expression (9, 10). Conversely, among the Aire^{+} mTECs, 60.2% expressed GAD67 and the rest did not, suggesting that Aire expression is not sufficient for TRA expression, at least for this Aire-independent TRA gene.

Expression of *Aire* and Aire-independent TRA genes by nonproliferating mTECs

Previous studies suggested that Aire is predominantly expressed by terminally differentiated cells on the basis of their poor incorporation of BrdU (26, 27). We confirmed this finding by injecting BrdU into *Aire*$^{+/gfp}$ mice. BrdU incorporation was scarce in GFP^{+} mTECs (Fig. 7 A, top). We similarly examined which type of mTECs, immature proliferating or mature nonproliferating, express GAD67 by injecting BrdU into GAD67/GFP knock-in mice. We found that GFP^{+} mTECs incorporated BrdU only weakly (Fig. 7 A, bottom), suggesting that expression of this Aire-independent TRA gene is also imposed on terminally differentiated cells rather on immature proliferating mTECs.

p63 is strongly expressed in epithelial stem cells of the thymus and specifically functions to maintain their extraordinary proliferative capacity (28). To examine whether mTECs expressing the *Aire* and *GAD67* genes have this high proliferative capacity, we examined p63 expression from thymi of Aire/GFP knock-in and GAD67/GFP knock-in adult mice. mTECs expressing GFP from both mouse strains showed little p63 expression by immunohistochemistry (Fig. 7 B), suggesting that neither of these genes is expressed in mTECs with high proliferative capacity. Instead, Aire seems to function within mTECs in the later stages of differentiation, when the cells are also responsible for TRA gene expression.

DISCUSSION

In the present study, we addressed fundamental questions regarding how mTECs acquire the capacity for promiscuous gene expression with the participation of Aire, with the hope that understanding the roles of Aire in thymic organogenesis will help to unravel the molecular mechanisms responsible for expression of immunological self in the thymic microenvironment. The issues include the following: first, whether Aire itself is necessary for the production and/or differentiation

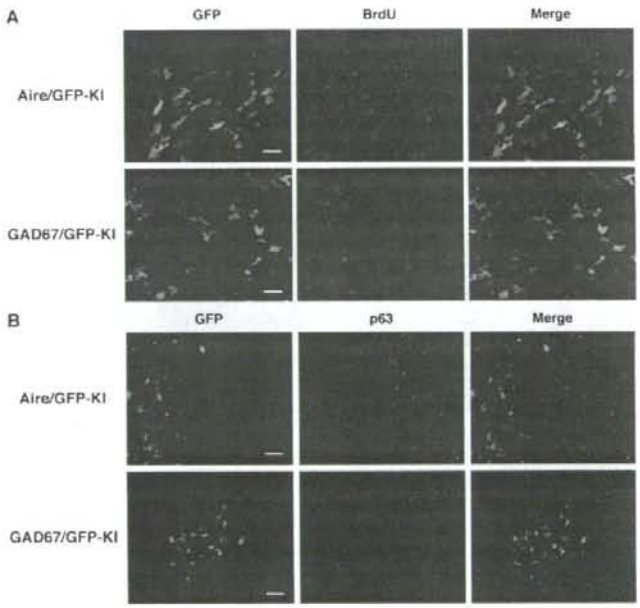

Figure 7. Expression of the *Aire* and *GAD67* genes by nonproliferating mTECs. (A) BrdU incorporation by *Aire*- and *GAD67*-expressing mTECs was evaluated 4 h after i.p. injection of BrdU into *Aire*$^{+/gfp}$ and *GAD67*$^{+/gfp}$ mice, respectively. The thymus sections were stained with anti-GFP (green) and anti-BrdU (red) Abs. Bars, 20 µm. (B) p63 (red) was not detected in mTECs expressing the *Aire* and *GAD67* genes (green). Bars, 40 µm. One representative experiment from a total of four repeats is shown.

Published November 17, 2008

program of Aire$^+$ cell lineages; second, whether Aire$^+$ mTECs are necessary for the structural and/or functional organization of other types of mTECs; third, to what extent Aire$^+$ mTECs contribute to the expression of TRA genes; and fourth, the nature of the maturation status of mTECs that express Aire and are responsible for TRA expression. Because Aire-specific Ab cannot be used to investigate the differentiation process of mTECs committed to express Aire in the absence of Aire protein, we established Aire/GFP knock-in mice in which the GFP marker gene was inserted into the *Aire* gene locus in a manner allowing concomitant disruption of functional Aire protein expression. In *Aire*$^{+/gfp}$ mice, this strategy also enables us to distinguish Aire-expressing cells from Aire-nonexpressing cells without introducing any cell markers incompletely unique to Aire-expressing cells. Accordingly, mTECs committed to Aire expression were faithfully GFP marked with this strategy; mTECs transcriptionally active for the *Aire* gene were mostly positive for staining with anti-Aire Ab by immunohistochemistry. There were, however, small numbers of cells that were either positive for Aire staining but negative for *Aire* gene transcription (i.e., GFP$^-$) or, conversely, positive for *Aire* gene transcription (i.e., GFP$^+$) but negative for Aire staining. The former cell type could result from different half-lives of the two proteins (GFP vs. Aire), whereas the latter cell type could result from Aire protein being present as a diffuse nucleoplasmic form (more difficult to recognize) instead of the typical nuclear-dot form (29). Alternatively, these discrepancies could simply be accounted for by differences in detection sensitivity. Indeed, RT-PCR analysis of flow cytometry–sorted cell fractions showed the expected patterns of *Aire* gene expression.

With Aire/GFP knock-in mice, we have clearly demonstrated that Aire$^+$ mTECs are the major cell types responsible for the expression of so-called Aire-dependent TRA genes such as *insulin 2* and *SAP1* (9, 10). These genes were almost exclusively expressed from GFP$^+$ mTECs of *Aire*$^{+/gfp}$ mice but not of *Aire*$^{gfp/gfp}$ mice. In contrast, expression of Aire-independent genes, such as *CRP*, was not affected by the absence of Aire. *CRP* expression from GFP$^+$ cells was similar between *Aire*$^{+/gfp}$ and *Aire*$^{gfp/gfp}$ mice. *CRP* expression, although at lower levels, was also observed from GFP$^-$ cells and, again, was indistinguishable between *Aire*$^{+/gfp}$ and *Aire*$^{gfp/gfp}$ mice. Expression of *GAD67* in an Aire-independent manner (9, 10) was also supported by immunohistochemistry of GAD67/GFP knock-in thymus, demonstrating *GAD67* expression irrespective of the presence of Aire protein in each mTEC. We speculate that the Aire dependency of TRAs reflects, in part, the cell types in which TRAs are expressed; expression of Aire-dependent genes is confined to Aire$^+$ mTECs, whereas expression of Aire-independent genes occurs from both Aire$^+$ and Aire$^-$ mTECs. It is of note that mTECs do not uniformly express the overlapping spectrum of TRAs, as exemplified by the scattered expression of the *GAD67* gene in GAD67/GFP knock-in mouse thymus. Similarly, although Aire$^+$ mTECs are the major cell types responsible for the expression of Aire-dependent TRA genes, this does not mean that all Aire$^+$ mTECs express Aire-dependent TRA genes uniformly. Indeed, single-cell analysis has demonstrated that expression of Aire in mTECs is not sufficient for simultaneous coexpression of Aire-dependent TRA genes (17). Thus, we favor the notion that promiscuous gene expression reflects the thymus-wide summation of expression of a small number of self-Ags by individual mTECs rather than expression of the complete spectrum of self-Ags by each cell (17, 18).

Because expression of transcription factors associated with developmental plasticity of progenitor cells (i.e., *Nanog*, *Oct4* and *Sox2*) is Aire-dependent in mTECs (18), the developmental model predicts that Aire acts early in the development of mTECs. The developmental model also suggests that promiscuous gene expression represents coordinated gene expression reflecting an alternate program of epithelial differentiation among actively proliferating mTECs at their progenitor or immature stages (19). However, accumulating data together with the results of the present study do not support such a view (26, 27). Rather, it is likely that Aire is acting at the late differentiation stages of mTECs. Accordingly, Aire-dependent processes for achieving promiscuous gene expression might also be active at the late differentiation stages of mTECs (see the subsequent paragraph). Clearly, this does not involve mTECs gaining the ability to express CD80 from CD80^{lo} precursors (30) because GFP$^+$ mTECs from *Aire*$^{gfp/gfp}$ mice demonstrated normal levels of CD80 expression. It is necessary to dissect the developmental process of mTECs, thereby precisely identifying the Aire-dependent steps of mTEC differentiation.

Given that Aire-expressing cells are terminally differentiated, the demonstration that Aire$^+$ mTECs are the major cell types responsible for expression of TRA genes, at least for Aire-dependent genes, apparently favors the terminal differentiation model for Aire-dependent promiscuous gene expression from mTECs (7, 10, 11). However, our results do support a key aspect of a role for Aire in the developmental model (17–19): absence of Aire in mTECs causes morphological changes together with altered distribution of mTECs committed to express Aire. Indeed, the difference in appearance of GFP-expressing cells was distinct enough to allow discrimination between *Aire*$^{+/gfp}$ and *Aire*$^{gfp/gfp}$ mouse sections by blind analysis. Interestingly, Gillard et al. (18) noted that globular mTECs without visible cellular projections were more prominent in Aire-deficient thymus, which could represent the GFP$^+$ globular mTECs we observed in *Aire*$^{gfp/gfp}$ mice. Furthermore, expression of functional molecules, such as CD80 and MHC class II from mTECs noncommitted to express Aire, was also affected by the absence of Aire, suggesting that Aire and/or Aire$^+$ mTECs influence the organization of mTECs beyond simply controlling promiscuous gene expression within Aire-expressing cell lineages. We do not believe that the demonstration that terminally differentiated Aire-expressing cells are the major source of promiscuous gene expression (apparently favoring the terminal differentiation model) and the demonstration that Aire and/or Aire$^+$ cells controls thymic organogenesis (consistent with the developmental model; reference 18 and present study) are mutually exclusive. Instead,

Aire could both promote the differentiation program of mTECs committed to express Aire, ensuring that they become fully equipped with the necessary machinery for promiscuous gene expression, and be an efficient driver of promiscuous gene expression in such cells. Thus, promiscuous gene expression seems to be accomplished in terminally differentiated mTECs that have matured in the presence of Aire protein (Fig. 8). Alternatively, Aire might be necessary for maintenance of a terminally differentiated state in which mTECs manifest a dendritic shape with fully competent promiscuous gene expression.

We found that the numbers of mTECs expressing involucrin, a marker of epidermal differentiation (22), were reduced in Aire-deficient mouse thymus. It was noteworthy that involucrin-expressing mTECs themselves were negative for Aire expression with immunohistochemistry (unpublished data), thus making it unlikely that *involucrin* gene expression in mTECs is under direct transcriptional control by Aire as a part of TRA gene expression. Similarly, it is unknown whether impaired involucrin expression is specific to mTECs committed to Aire expression or whether lack of Aire$^+$ mTECs affects the differentiation of other type(s) of mTECs that would otherwise express involucrin at their terminally differentiated stages. Based on the fact that GFP$^+$ Aire-less mTECs showed alterations in their morphology as well as distribution, we assume that the former possibility is more likely. Interestingly,

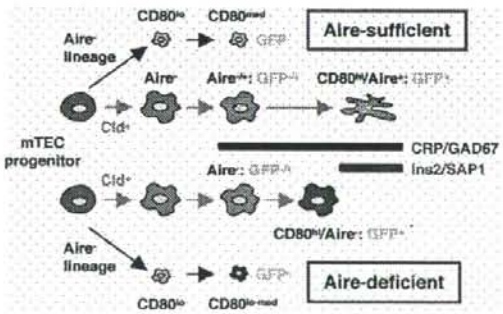

Figure 8. Schematic representation of the roles of Aire in mTEC differentiation and TRA gene expression. Aire-expressing cell lineages develop from mTEC progenitor cells through concomitant expression of claudin (26). Expression of Aire-dependent TRA genes, such as *insulin 2* and *SAP1*, can be accomplished in terminally differentiated mTECs showing a dendritic to fibroblastic morphology that have fully matured with the help of Aire protein (marked as Aire-sufficient). Lack of Aire in mTECs results in premature termination of differentiation, although claudin$^+$ Aire-expressing cell lineages can still develop and pass the CD80-expressing maturation stage (marked as Aire-deficient). These CD80^{lo} Aire-less mTECs have a more globular cell shape and lack transcriptional machinery for Aire-dependent TRA genes. Because Aire-independent TRA genes, such as *CRP* and *GAD67*, can be expressed before the terminal differentiation stages, lack of Aire has little impact on their expression. The possibility also remains that Aire is necessary for the maintenance of a terminally differentiated state, in which mTECs manifest a dendritic shape with fully competent promiscuous gene expression.

we found that reduction of involucrin-expressing mTECs in Aire-deficient mice was associated with a nearly absence of Hassall's corpuscle-like structures, although the exact relevance of this phenotype to the breakdown of central tolerance in Aire-deficient mice remains unknown (31). Together with the fact that formation of thymic cysts is a predominant feature of Aire-deficient mice (18, 26), it seems likely that Aire exerts more global control of the differentiation program of mTECs than was initially thought.

Finally, although we have demonstrated that Aire organizes the global mTEC integrity that facilitates promiscuous gene expression in the thymic microenvironment, the exact nature of the mTEC differentiation program under the control of Aire protein still remains unknown. We have demonstrated that both *Aire* and an Aire-independent TRA gene, *GAD67*, are predominantly expressed by nonproliferative cells, although we cannot completely exclude the possibility that expression of these genes is associated with immature cells that turn over slowly and, thus, would be poorly labeled by BrdU. The results prompt us to propose a fascinating hypothesis that promiscuous gene expression is achieved by induction of heterogeneity among terminally differentiated mTECs rather than by multipotentiality of mTEC progenitors. We speculate that Aire may contribute to mTEC heterogeneity by acting on mTECs at the late differentiation stages and that lack of Aire may result in failure to create this heterogeneity. According to this scenario, additional mechanisms for the development of Aire-dependent autoimmunity might be possible beyond reduced TRA expression from Aire-deficient mTECs, for instance, altered Ag processing and/or presentation capacity by Aire-deficient mTECs (12) and/or altered T cell development affecting establishment of the complete T cell repertoire. Study of the mechanisms underlying the Aire-dependent production of heterogeneity among mature mTECs might be a rewarding approach to elucidating the nature of the negative selection niche in the thymus.

MATERIALS AND METHODS

Mice. Aire/GFP knock-in mice (RIKEN Center for Developmental Biology accession No. CDB0483K) were generated by gene targeting as described previously (32). In brief, the targeting vector was constructed by replacing the genomic *Aire* locus starting from exon 1 (immediately after the Kozak sequence) to exon 2 with a GFP-neomycin resistance (neo^r) gene cassette (20). The neo^r gene cassette harbors loxP sites at both ends. The targeting vector was introduced into TT2 embryonic stem cells (33), and the homologous recombinant clones were first identified by PCR and confirmed by Southern blot analysis. After the targeted cells had been injected into morula-stage embryos, the resulting chimeric male mice were mated with C57BL/6 females (CLEA) to establish germ-line transmission. $Aire^{+/gfp\text{-}neo}$ mice were crossed with Ayu1-Cre mice (21), a general deleter Cre recombinase-expressing transgenic line, to remove the neo^r gene cassette. After confirming removal of the neo^r gene cassette, mice were crossed with C57BL/6 mice to select the line containing the GFP knock-in allele but not the Cre recombinase-expressing transgene. $Aire^{+/gfp}$ mice were then crossed to obtain $Aire^{gfp/gfp}$ mice, which have the null mutation for the *Aire* gene. GAD67/GFP knock-in mice were heterozygous for GAD67-GFP (Δneo) as described previously (34). OT-II transgenic mice (35) were purchased from The Jackson Laboratory. The mice were maintained under pathogen-free conditions.

Published November 17, 2008

The protocols used in this study were in accordance with the Guidelines for Animal Experimentation of Tokushima University School of Medicine and were conducted with the approval of the RIKEN Kobe Animal Experiment Committee.

Immunohistochemistry. Mice were killed and the thymus tissues were fixed as described previously (25, 36). Immunohistochemical analysis of the thymus with UEA-1 (Vector Laboratories), rat anti-EpCAM mAb (BD), and rabbit polyclonal anti-K5 Ab (Covance) was performed as described previously (37). Rabbit polyclonal anti-Aire Ab was produced as described previously (13). Goat polyclonal anti-GFP Ab (Novus Biologicals) and rabbit polyclonal anti-GFP Ab (Invitrogen) were used for the detection of GFP-expressing cells. BrdU incorporation by mTECs was examined 4 h after i.p. injection of 1 mg BrdU/mouse, and the detection of BrdU incorporation was performed with anti-BrdU Ab (BD), as described previously (26). Rabbit polyclonal anti-p63 Ab was purchased from Santa Cruz Biotechnology, Inc. The level of cell shape complexity for each GFP$^+$ cell was calculated by dividing the length of the cellular periphery by the cell area (i.e., periphery/area $\times$ $1/4\pi$) measured by the WinROOF program (Mitani Corporation). After obtaining photos of the thymus sections stained with anti-GFP Ab, the photos were subjected to analysis with the software. Immunohistochemistry of the thymus sections and statistical analysis of cell shape complexity from different genotype of mice for comparison were processed simultaneously in the same set of experiment to minimize variability between the assays. Numbers of involucrin-expressing mTECs were assessed after staining the thymus sections with rabbit polyclonal Ab against mouse involucrin (Covance). Well developed EpCAM$^+$ thymic medullas were examined for the presence of involucrin-expressing cells from several thymus sections obtained from individual mice.

TEC preparation and flow cytometric analysis. TECs were prepared as described previously (12). In brief, thymic lobes were isolated from mice and cut into small pieces. The fragments were gently rotated in RPMI 1640 medium (Invitrogen) supplemented with 10% heat-inactivated FCS (Invitrogen), 20 mM Hepes, 100 U/ml penicillin, 100 μg/ml streptomycin, and 50 μM 2-ME at 4°C for 30 min and dispersed further with pipetting to remove the majority of thymocytes. The resulting thymic fragments were digested with 0.125% collagenase D (Roche) and 10 U/ml DNase I (Roche) in RPMI 1640 at 37°C for 15 min. The supernatants, containing dissociated TECs, were saved, and the remaining thymic fragments were further digested with collagenase D and DNase I. This step was repeated twice, and the remaining thymic fragments were digested with 0.125% collagenase/dispase (Roche) and DNase I at 37°C for 30 min. The supernatants from this digest were combined with the supernatants from the collagenase digests, and the mixture was centrifuged for 5 min at 450 *g*. The cells were suspended in PBS, containing 5 mM EDTA and 0.5% FCS, and kept on ice until the staining. The cells were stained with anti-CD45 mAb (BD) and UEA-1 and subjected to flow cytometric cell sorting with a FACS Vantage (BD). Flow cytometric analysis was performed after staining the cells with anti-CD45 mAb, UEA-1, anti-I-A^b (eBioscience), and anti-CD80 (eBioscience) mAbs with a FACSCalibur (BD) as described previously (13, 37).

Real-time PCR. RNA was extracted from sorted mTECs with RNeasy Mini kits (QIAGEN) and made into cDNA with cDNA Cycle kits (Invitrogen) according to the manufacturer's instructions. Real-time PCR for quantification of the *insulin 2*, *SAP1*, *CRP*, and *Hprt* genes was performed as described previously (12, 13). The primers and the probes are as follows: *insulin 2* primers, 5′-AGACCATCAGCAAGCAGGTC-3′ and 5′-CTGGTGCAGCACTGATCCAC-3′; *insulin 2* probe, 5′-FAM-CCCGGCAGAAGCGTGGCATT-3′; *SAP1* primers, 5′-ACTCCTTGTGTTGCTTGGTGTTT-3′ and 5′-TCGACTGAATCAGAGGAATCAACT-3′; *SAP1* probe, 5′-FAM-TTCACCAGCAGAATCAGCAGTTCCAGAA-3′; *CRP* primers, 5′-TACTCTGGTGCCTTCTGATCATGA-3′ and 5′-GGCTTCTTTGACTCTGCTTCCA-3′; *CRP* probe, 5′-FAM-CAGCTTCTCTCGGACTTTTGGTCATGA-3′; *Hprt* primers, 5′-TGAAGAGCTACTGTAATGATCAGTCAAC-3′ and 5′-AGCAAGCTTGCAACCTTAACCA-3′; and *Hprt* probe, 5′-FAM-TGCTTTCCCTGGTTAAGCAGTACAGCCC-3′.

Statistical analysis. All results are expressed as mean ± SEM. Statistical analysis was performed using Student's two-tailed unpaired *t* test for comparisons between two groups. Differences were considered significant if p-values were 0.05 or less.

Online supplemental materials. Fig. S1 shows Aire-expressing cells in adult and embryonic thymi. Fig. S2 shows altered morphology together with the distribution of GFP$^+$ Aire-less mTECs in *Aire*^{gfp} mice. Fig. S3 shows altered morphology together with the distribution of GFP$^+$ Aire-less mTECs in *Aire*$^{-/gfp}$ mice expressing the nonautoreactive OT-II TCR transgene. Fig. S4 shows altered morphology of GFP$^+$ Aire-less mTECs in *Aire*$^{gfp/gfp}$ mice at neonatal stage P1. Table S1 shows detailed information for mice analyzed for involucrin-expressing mTECs. Online supplemental material is available at http://www.jem.org/cgi/content/full/jem.20080046/DC1.

We thank Drs. Y. Hamazaki, E.A. Robey and A.G. Farr for suggestions on immunohistochemistry.

This work was supported in part by Grants-in-Aid for Scientific Research from the Japan Society for the Promotion of Science and from the Ministry of Education, Culture, Sports, Science and Technology of Japan, and by Health and Labor Sciences Research Grants, Research on Psychiatric and Neurological Diseases and Mental Health (M. Matsumoto).

The authors have no conflicting financial interests.

Submitted: 7 January 2008
Accepted: 17 October 2008

REFERENCES

1. Kamradt, T., and N.A. Mitchison. 2001. Tolerance and autoimmunity. *N. Engl. J. Med.* 344:655–664.
2. Björses, P., J. Aaltonen, N. Horelli-Kuitunen, M.L. Yaspo, and L. Peltonen. 1998. Gene defect behind APECED: a new clue to autoimmunity. *Hum. Mol. Genet.* 7:1547–1553.
3. Pitkänen, J., and P. Peterson. 2003. Autoimmune regulator: from loss of function to autoimmunity. *Genes Immun.* 4:12–21.
4. Björses, P., M. Pelto-Huikko, J. Kaukonen, J. Aaltonen, L. Peltonen, and I. Ulmanen. 1999. Localization of the APECED protein in distinct nuclear structures. *Hum. Mol. Genet.* 8:259–266.
5. Heino, M., P. Peterson, J. Kudoh, K. Nagamine, A. Lagerstedt, V. Ovod, A. Ranki, I. Rantala, M. Nieminen, J. Tuukkanen, et al. 1999. Autoimmune regulator is expressed in the cells regulating immune tolerance in thymus medulla. *Biochem. Biophys. Res. Commun.* 257:821–825.
6. Hogquist, K.A., T.A. Baldwin, and S.C. Jameson. 2005. Central tolerance: learning self-control in the thymus. *Nat. Rev. Immunol.* 5:772–782.
7. Kyewski, B., and L. Klein. 2006. A central role for central tolerance. *Annu. Rev. Immunol.* 24:571–606.
8. Derbinski, J., A. Schulte, B. Kyewski, and L. Klein. 2001. Promiscuous gene expression in medullary thymic epithelial cells mirrors the peripheral self. *Nat. Immunol.* 2:1032–1039.
9. Anderson, M.S., E.S. Venanzi, L. Klein, Z. Chen, S.P. Berzins, S.J. Turley, H. von Boehmer, R. Bronson, A. Dierich, C. Benoist, and D. Mathis. 2002. Projection of an immunological self shadow within the thymus by the aire protein. *Science.* 298:1395–1401.
10. Derbinski, J., J. Gabler, B. Brors, S. Tierling, S. Jonnakuty, M. Hergenhahn, L. Peltonen, J. Walter, and B. Kyewski. 2005. Promiscuous gene expression in thymic epithelial cells is regulated at multiple levels. *J. Exp. Med.* 202:33–45.
11. Liston, A., D.H. Gray, S. Lesage, A.L. Fletcher, J. Wilson, K.E. Webster, H.S. Scott, R.L. Boyd, L. Peltonen, and C.C. Goodnow. 2004. Gene dosage–limiting role of *Aire* in thymic expression, clonal deletion, and organ-specific autoimmunity. *J. Exp. Med.* 200:1015–1026.
12. Kuroda, N., T. Mitani, N. Takeda, N. Ishimaru, R. Arakaki, Y. Hayashi, Y. Bando, K. Izumi, T. Takahashi, T. Nomura, et al. 2005. Development

Published November 17, 2008

JEM

of autoimmunity against transcriptionally unrepressed target antigen in the thymus of Aire-deficient mice. *J. Immunol.* 174:1862–1870.

13. Niki, S., K. Oshikawa, Y. Mouri, F. Hirota, A. Matsushima, M. Yano, H. Han, Y. Bando, K. Izumi, M. Matsumoto, et al. 2006. Alteration of intra-pancreatic target-organ specificity by abrogation of Aire in NOD mice. *J. Clin. Invest.* 116:1292–1301.
14. Anderson, M.S., E.S. Venanzi, Z. Chen, S.P. Berzins, C. Benoist, and D. Mathis. 2005. The cellular mechanism of Aire control of T cell tolerance. *Immunity.* 23:227–239.
15. Devoss, J., Y. Hou, K. Johannes, W. Lu, G.I. Liou, J. Rinn, H. Chang, R. Caspi, L. Fong, and M.S. Anderson. 2006. Spontaneous autoimmunity prevented by thymic expression of a single self-antigen. *J. Exp. Med.* 203:2727–2735.
16. Matsumoto, M. 2007. Transcriptional regulation in thymic epithelial cells for the establishment of self tolerance. *Arch. Immunol. Ther. Exp. (Warsz.).* 55:27–34.
17. Gillard, G.O., and A.G. Farr. 2006. Features of medullary thymic epithelium implicate postnatal development in maintaining epithelial heterogeneity and tissue-restricted antigen expression. *J. Immunol.* 176:5815–5824.
18. Gillard, G.O., J. Dooley, M. Erickson, L. Peltonen, and A.G. Farr. 2007. Aire-dependent alterations in medullary thymic epithelium indicate a role for Aire in thymic epithelial differentiation. *J. Immunol.* 178:3007–3015.
19. Gillard, G.O., and A.G. Farr. 2005. Contrasting models of promiscuous gene expression by thymic epithelium. *J. Exp. Med.* 202:15–19.
20. Moriguchi, T., M. Hamada, N. Morito, T. Terunuma, K. Hasegawa, C. Zhang, T. Yokomizo, R. Esaki, E. Kuroda, K. Yoh, et al. 2006. Mafb is essential for renal development and F4/80 expression in macrophages. *Mol. Cell. Biol.* 26:5715–5727.
21. Niwa, H., K. Araki, S. Kimura, S. Taniguchi, S. Wakasugi, and K. Yamamura. 1993. An efficient gene-trap method using poly A trap vectors and characterization of gene-trap events. *J. Biochem.* 113:343–349.
22. Fuchs, E. 1990. Epidermal differentiation. *Curr. Opin. Cell Biol.* 2:1028–1035.
23. Hale, L.P., and M.L. Markert. 2004. Corticosteroids regulate epithelial cell differentiation and Hassall body formation in the human thymus. *J. Immunol.* 172:617–624.
24. Patel, D.D., L.P. Whichard, G. Radcliff, S.M. Denning, and B.F. Haynes. 1995. Characterization of human thymic epithelial cell surface antigens: phenotypic similarity of thymic epithelial cells to epidermal keratinocytes. *J. Clin. Immunol.* 15:80–92.
25. Maemura, K., Y. Yanagawa, K. Obata, T. Dohi, Y. Egashira, Y. Shibayama, and M. Watanabe. 2006. Antigen-presenting cells expressing glutamate decarboxylase 67 were identified as epithelial cells in glutamate decarboxylase 67-GFP knock-in mouse thymus. *Tissue Antigens.* 67:198–206.
26. Hamazaki, Y., H. Fujita, T. Kobayashi, Y. Choi, H.S. Scott, M. Matsumoto, and N. Minato. 2007. Medullary thymic epithelial cells expressing Aire represent a unique lineage derived from cells expressing claudin. *Nat. Immunol.* 8:304–311.
27. Gray, D., J. Abramson, C. Benoist, and D. Mathis. 2007. Proliferative arrest and rapid turnover of thymic epithelial cells expressing Aire. *J. Exp. Med.* 204:2521–2528.
28. Senoo, M., F. Pinto, C.P. Crum, and F. McKeon. 2007. p63 Is essential for the proliferative potential of stem cells in stratified epithelia. *Cell.* 129:523–536.
29. Akiyoshi, H., S. Hatakeyama, J. Pitkänen, Y. Mouri, V. Doucas, J. Kudoh, K. Tsurugaya, D. Uchida, A. Matsushima, K. Oshikawa, et al. 2004. Subcellular expression of autoimmune regulator (AIRE) is organized in a spatiotemporal manner. *J. Biol. Chem.* 279:33984–33991.
30. Rossi, S.W., M.Y. Kim, A. Leibbrandt, S.M. Parnell, W.E. Jenkinson, S.H. Glanville, F.M. McConnell, H.S. Scott, J.M. Penninger, E.J. Jenkinson, et al. 2007. RANK signals from CD4^{+}3^{-} inducer cells regulate development of Aire-expressing epithelial cells in the thymic medulla. *J. Exp. Med.* 204:1267–1272.
31. Liu, Y.J. 2006. A unified theory of central tolerance in the thymus. *Trends Immunol.* 27:215–221.
32. Murata, T., K. Furushima, M. Hirano, H. Kiyonari, M. Nakamura, Y. Suda, and S. Aizawa. 2004. *ang* is a novel gene expressed in early neuroectoderm, but its null mutant exhibits no obvious phenotype. *Gene Expr. Patterns.* 5:171–178.
33. Yagi, T., T. Tokunaga, Y. Furuta, S. Nada, M. Yoshida, T. Tsukada, Y. Saga, N. Takeda, Y. Ikawa, and S. Aizawa. 1993. A novel ES cell line, TT2, with high germline-differentiating potency. *Anal. Biochem.* 214:70–76.
34. Tamamaki, N., Y. Yanagawa, R. Tomioka, J. Miyazaki, K. Obata, and T. Kaneko. 2003. Green fluorescent protein expression and colocalization with calretinin, parvalbumin, and somatostatin in the GAD67-GFP knock-in mouse. *J. Comp. Neurol.* 467:60–79.
35. Barnden, M.J., J. Allison, W.R. Heath, and F.R. Carbone. 1998. Defective TCR expression in transgenic mice constructed using cDNA-based alpha- and beta-chain genes under the control of heterologous regulatory elements. *Immunol. Cell Biol.* 76:34–40.
36. Kusser, K.L., and T.D. Randall. 2003. Simultaneous detection of EGFP and cell surface markers by fluorescence microscopy in lymphoid tissues. *J. Histochem. Cytochem.* 51:5–14.
37. Kajiura, F., S. Sun, T. Nomura, K. Izumi, T. Ueno, Y. Bando, N. Kuroda, H. Han, Y. Li, A. Matsushima, et al. 2004. NF-κB-inducing kinase establishes self-tolerance in a thymic stroma-dependent manner. *J. Immunol.* 172:2067–2075.